



INDC(NDS)-0655
Distr. AI+MN+NM

INDC International Nuclear Data Committee

Summary Report

Third Research Coordination Meeting on

Prompt Fission Neutron Spectra of Major Actinides

IAEA Headquarters
Vienna, Austria
21 – 24 October 2013

Prepared by

Patrick Talou
Los Alamos National Laboratory
New Mexico, USA

R. Capote Noy
IAEA Nuclear Data Section
Vienna, Austria

S. Simakov
IAEA Nuclear Data Section
Vienna, Austria

December 2014

Selected INDC documents may be downloaded in electronic form from
<http://www-nds.iaea.org/publications>
or sent as an e-mail attachment.

Requests for hardcopy or e-mail transmittal should be directed to
NDS.Contact-Point@iaea.org

or to:

Nuclear Data Section
International Atomic Energy Agency
Vienna International Centre
PO Box 100
1400 Vienna
Austria

Printed by the IAEA in Austria

February 2015

Summary Report

Third Research Coordination Meeting on

Prompt Fission Neutron Spectra of Major Actinides

IAEA Headquarters
Vienna, Austria
21 – 24 October 2013

Prepared by

Patrick Talou
Los Alamos National Laboratory
New Mexico, USA

R. Capote Noy
IAEA Nuclear Data Section
Vienna, Austria

S. Simakov
IAEA Nuclear Data Section
Vienna, Austria

Abstract

A summary is given of the Third Research Coordination Meeting on Prompt Fission Neutron Spectra of Actinides. Experimental data, modelling and evaluation methods on prompt fission neutron spectra were reviewed. Extensive technical discussions were held on theoretical methods to calculate prompt fission spectra, and on uncertainty analysis of experimental data. Summary reports of selected technical presentations at the meeting are given. All presentations are available online at <https://www-nds.iaea.org/index-meeting-crp/PFNS-3RCM/>. The resulting work plan of the Coordinated Research Programme preparing the final technical report is summarized, along with actions and deadlines.

December 2014

TABLE OF CONTENTS

1. Introduction	7
2. Technical document chapters	8
2.1 Experiments	8
2.2 Modeling	9
2.3 Evaluations (spectrum + covariances)	11
2.4 Data Testing	13
2.5 Open Questions	14
3. Conclusions	15
Appendix 1. Agenda	17
Appendix 2. List of participants	19
Appendix 3. Meeting photo	21
Appendix 4. Selected reports by meeting participants	23
1. Total prompt fission neutron spectrum from thermal-neutron-induced fission of ^{235}U , A.S. Vorobyev and O. A. Shcherbakov	23
2. Model calculations of prompt fission neutron spectra of $^{232}\text{Th}(n,f)$, A. Tudora	32

1. Introduction

The energy spectrum of prompt neutrons emitted in fission plays an important role in many applications in nuclear science and technology, including reactor applications, criticality and benchmarking calculations. While the accuracy of fission cross sections and neutron multiplicities (ν_{bar}) in the relevant energy range has been steadily improved and is well below 1%, we are faced with the situation that existing measured prompt fission neutron spectra (PFNS) are in many cases discrepant, and that different PFNS theoretical models give differing predictions. The conclusion from the Consultants' Meeting on Prompt Fission Neutron Spectra of Major Actinides, which was held at the IAEA Headquarters in Vienna, Austria, in November 2008 and summarized in a report [1] was that the PFNS in the present evaluated nuclear data libraries are inadequate and that their uncertainty estimates are unrealistic.

As a consequence, a Coordinated Research Project (CRP) on Prompt Fission Neutron Spectra for Actinides was initiated by the IAEA in 2010. The proposed goal was to determine the prompt fission neutron spectra and covariance matrices for actinides in the energy range from thermal to 20 MeV. Its first Research Coordination Meeting (RCM) was held at IAEA Headquarters, Vienna, Austria from 6 to 9 April 2010. Experimental data and modelling methods on prompt fission neutron spectra were reviewed. The programme to compile and evaluate prompt fission spectra including uncertainty information over the neutron energy range from thermal to 20 MeV was proposed. A summary report of that meeting was published as an IAEA(NDS)-0571 technical report [2]. The Second Research Coordination Meeting of the CRP was held at IAEA Headquarters, Vienna, Austria from 13 to 16 December 2011 and was attended by fifteen CRP participants. A summary report of that meeting was published as an IAEA(NDS)-0608 technical report [3].

At the same time, significant efforts have been made by the Neutron Standards Evaluation Group to undertake a new evaluation of the PFNS in the thermal-neutron-induced fission of the ^{235}U nucleus that could be proposed as a secondary reference neutron spectrum. The ongoing work is summarized in meeting reports by Pronyaev et al [4,5].

The Third Research Coordination Meeting of the CRP named Prompt Fission Neutron Spectra for Actinides was held at IAEA Headquarters, Vienna, Austria from 21 to 24 October 2013 and was attended by twelve CRP participants. The IAEA was represented by S. Simakov, N. Otsuka and R. Capote, who served as Scientific Secretary. N. Kornilov (Ohio University, USA) was elected Chairman of the meeting and P. Talou (LANL, USA) agreed to act as rapporteur. The approved Agenda is attached as Appendix 1, the list of participants and their affiliations as Appendix 2 and the meeting photo as Appendix 3. The following nuclei have been studied within the CRP:

- major actinides $^{235,238}\text{U}$ and ^{239}Pu ;
- ^{232}Th , ^{233}U , and ^{234}U of relevance to the Th-U fuel cycle;

Additionally evaluations will be also available for all remaining nuclei in the uranium and

¹ R. Capote, V. Maslov, E. Bauge, T. Ohsawa, A. Vorobyev, M.B. Chadwick and S. Oberstedt, *Summary Report of Consultants' Meeting on Prompt Fission Neutron Spectra of Major Actinides*, INDC(NDS)-0541 (IAEA, Vienna, Austria, 2009) at <https://www-nds.iaea.org/publications/indc/indc-nds-0541.pdf>.

² R. Capote Noy, *Summary Report of the First Research Coordination Meeting on Prompt Fission Neutron Spectra of Major Actinides*, INDC(NDS)-0571 (IAEA, Vienna, Austria, 2010) at <https://www-nds.iaea.org/publications/indc/indc-nds-0571.pdf>.

³ R. Capote Noy, *Summary Report of the Second Research Coordination Meeting on Prompt Fission Neutron Spectra of Major Actinides*, INDC(NDS)-0608 (IAEA, Vienna, Austria, 2011) at <https://www-nds.iaea.org/publications/indc/indc-nds-0608.pdf>.

⁴ V.G. Pronyaev, A.D. Carlson, R. Capote and A. Wallner, *Summary Report of Consultants' Meeting on International Cross-Section Standards: Extending and Updating*, INDC(NDS)-0583 (IAEA, Vienna, 2011) at <https://www-nds.iaea.org/publications/indc/indc-nds-0583.pdf>.

⁵ V.G. Pronyaev, A.D. Carlson and R. Capote Noy, *Toward a New Evaluation of Neutron Standards*, INDC(NDS)-0641, (IAEA, Vienna, Austria, 2013) at <https://www-nds.iaea.org/publications/indc/indc-nds-0641.pdf>.

plutonium isotopic chains. Selected reports by meeting participants including relevant figures are attached as Appendix 4. All presentations at the meeting are available online at <https://www-nds.iaea.org/index-meeting-crp/PFNS-3RCM/>.

A detailed list of actions to be undertaken toward producing a final technical document is given in the next Section.

2. Technical document chapters

2.1 Experiments

Actions:

- **All:** Produce complete list of experiments
 - **Capote:** Provide preliminary files (x,y,dy) for all experiments/isotopes plus PDF of references on web site
 - Provide updated files (x,y,dy,dy1,dy2,...)
 - **All:** Provide draft Section to Roberto
 - Isotopes of interest for full covariance analysis: U235all, Pu239all, U238, Th232
 - Less-important isotopes: U233
 - Check EXFOR entries for description on uncertainty estimation
 - Request missing documents
 - Detailed experiment description: emphasis on sources of systematic uncertainties
 - Stability, detector thresholds, ...
 - Table with a list of: experimental details like detector type, flight path, time resolution, efficiency determination – either absolute or relative, fission trigger, sample characteristics, multiple scattering, angular information with respect to fission and neutron emission, bin-width correction, time resolution correction, etc
 - Rejection of data sets? Include a recommendation in the table
 - Assess uncertainties quantitatively
 - Discuss inter-experiment correlation?
 - Overview of on-going experiments provided by each group member
 - Recommendations for future experiments.
 - Guideline on Uncertainty Quantification from Denise
 - Exchange of drafts
 - All drafts to SO
 - Homogenization of chapter (2) and submission to Denise
 - Exchange of opinions
 - Finalization of the document for submission
 - Submission of document to Roberto
1. List of all experiments, isotopes used in this study [add tables]
 - a. U235: thermal (6 data sets) [“standard”] and Cf252sf: “standard”
 - b. U235: all other energies
 - c. Pu239: thermal, up to 3.5 MeV + Chatillon Einc=1-60 MeV
 - d. U233: thermal, 0.5 MeV
 - e. U238: all energies
 - f. Th232: all energies
 - g. Minor Actinides: EXFOR data list (Otsuka)

Isotope	Incident Energy (MeV)	Source (EXFOR#, private comm., ...)	First Author	Year	Outgoing Energy Range	UQ	Main Reference
U235	thermal						
	0.5						

2. Each (important!) isotope: table including sources of uncertainties, corrections, etc.
 - U235, thermal: [Kornilov, Pronyaev \(Neudecker\)](#)
 - U235, other energies: [Kornilov](#)
 - Cf252sf: not considered, taken from Mannhart
 - Pu239, thermal, 0.215, 0.5-3.5: [Neudecker](#) (appendix, LA-UR...) + Chatillon?
 - U233: [Pronyaev, Vorobyev](#)
 - U238: [Oberstedt, Saxena](#)
 - Th232: [Saxena, Oberstedt](#)
 - Minor actinides (just a list of data sets): [IAEA](#)
3. Overview of ongoing or planned future experiments: Chi-Nu (LANSCE), U238 (Bruyeres-le-Chatel; BARC, India; IRMM?), Cf252sf (Eout>8 MeV; Ohio U.); Cf252sf (IRMM, Chi-Nu?)
4. Recommendations for future experiments, future detectors, etc. [Kornilov](#)
5. Web repository of experimental data sets with uncertainty quantification. [IAEA](#)
Common format for all experimental sets: (x,y,dy) to be used in comparison plots evaluations/experiments (see below).
(Mention if bin-width correction taken into account or not.)
6. Uncertainty quantification of experiments: write-up on the UQ methodology used for Chi-Nu data ([Neudecker](#))

2.2 Modeling

Actions:

- **Capote:**
 - Place fission fragment yields (Cf252sf, U235th, Pu239th, and Th232 at 2.0 MeV) on CRP web repository
 - Provide (web site) Nuclear Data Sheets template with agreed upon structure to be used for draft document
 - Write Section on “Two-Watt” model (with Kornilov)
- **Kornilov:**
 - Write FINE code description (~5 pages)
 - Compute U235th output for code inter-comparison (see below)
 - Perform “best” PFNS calculations for Cf252sf, U235th, Pu239th, Th232 (2.0 MeV)

- **Ohsawa:**
 - Write Los Alamos model Section
 - Perform “best” PFNS calculations for Cf252sf, U235th, Pu239th, Th232 (2.0 MeV)

- **Schmidt:**
 - Provide Th232 FF Yields at 2.0 MeV from GEF code
 - Write Section 1 draft (can we use what he already sent?)
 - Write GEF code description (~5 pages)
 - Compute U235th output for code inter-comparison (see below)
 - Perform “best” PFNS calculations for Cf252sf, U235th, Pu239th, Th232 (2.0 MeV)

- **Serot:**
 - Provide FF Yields from FIFRELIN for Cf252sf, U235th, Pu239th
 - Write FIFRELIN code description (~5 pages)
 - Compute U235th output for code inter-comparison (see below)
 - Perform “best” PFNS calculations for Cf252sf, U235th, Pu239th, Th232 (2.0 MeV)

- **Shu:**
 - Write Section on Semi-Empirical Model
 - Compute U235th output for code inter-comparison (see below)
 - Perform “best” PFNS calculations for Cf252sf and U235th

- **Talou:**
 - Provide FF Yields format template & write README
 - Provide FF Yields from CGMF for Cf252sf, U235th, Pu239th
 - Provide script to project FF Yields in $Y(A)$, $Y(TKE)$ and $\langle TKE \rangle(A)$
 - Write CGMF code description (~5 pages)
 - Write Introduction/Technical Framework to Monte Carlo codes
 - Compute U235th output for code inter-comparison (see below)
 - Collect all U235th results from code inter-comparisons and prepare tables/plots
 - Perform “best” PFNS calculations for Cf252sf, U235th, Pu239th, Th232 (2.0 MeV)

- **Tudora:**
 - Provide FF Yields for Cf252sf, U235th, Pu239th
 - Write PbP Section
 - Compute U235th output for code inter-comparison (see below)
 - Perform “best” PFNS calculations for Cf252sf, U235th, Pu239th, Th232 (2.0 MeV)

- **Vogt:**
 - Provide FF Yields for Cf252sf, U235th, Pu239th
 - Write FREYA code description (~5 pages)
 - Compute U235th output for code inter-comparison (see below)
 - Perform “best” PFNS calculations for Cf252sf, U235th, Pu239th, Th232 (2.0 MeV)

To be covered in **each model section**: physics assumptions, input data & model parameters, output data, sensitivity of calculated results to input data and model parameters. Calculations of selected spectra (Cf252sf, U235th, Pu239th).

1. Physics of nuclear fission starting near scission point, [Schmidt](#) (draft manuscript as starting point)
 - a. Fission fragment yields (A,Z,TKE) – web repository with yield data, [Talou](#) (provide scripts for projected distributions), [Capote](#)
 - b. Emissions from fully accelerated fragments, during the acceleration of fragments, at scission, before scission
 - c. Neutron-gamma competition
 - d. Excitation energy partitioning
 - e. Angular momentum in the fragments
 - f. Nuclear structure and level density of neutron-rich nuclei
2. Los Alamos model, [Ohsawa](#)
 - a. “Original” – main assumptions, input, output (average spectrum & multiplicity)
 - b. Newer developments: anisotropy, different temperatures, multi-modal fission, different multiplicities, ...
3. Point-by-Point, [Tudora](#)
 - a. Based on Los Alamos model for each fragment pair
 - b. Properties: level density, TXE partitioning, P(T) residual distribution, ...
4. SEM, [Shu](#)
5. Two-Watt “model” (Minsk library), [Kornilov](#), [Capote](#)
6. Monte Carlo
 - a. Technical framework (introduction to MC codes)
 - i. Sampling fission fragment yields (comparisons between different distributions)
 - ii. Sampling gamma and neutron emission probabilities
 - b. Codes
 - i. GEF, [Schmidt](#)
 - ii. FREYA, [Vogt](#)
 - iii. FIFRELIN, [Serot](#)
 - iv. CGMF, [Talou](#)
 - v. FINE, [Kornilov](#)
 - c. Code inter-comparison (*Use GEF FF yields of U235th*)
 - i. PFNS, $\langle v \rangle$, $P(v)$, $\langle E_{cm} \rangle$, $\langle E_{lab} \rangle$, $\langle v \rangle$ (TKE), $\langle v \rangle$ (A), ang. dist. n-LF
 - ii. Same for prompt gammas
7. Inter-comparison of “best” PFNS calculated by all models
 - a. Cf252sf, U235th, Pu239th
 - b. Th232 (2.0 MeV, yields to be provided by [Schmidt](#) or/and [Tudora](#))
 - c. U238 and Th232 at 7.0 and 14 MeV

2.3 Evaluations (spectrum + covariances)

Actions:

- [Talou](#): Provide updated evaluations U and Pu isotopes (normalization problem; naming convention)
- [Shu](#): Provide U235 evaluation in ENDF format (1st-chance fission)
- [Capote](#): Provide selected files from Minsk library
- [Morillon](#): Provide BRC evaluated files
- [Tudora](#): Provide Np237 evaluation file

- **Tudora**: Provide LA model input parameters to LANL
 - **Vogt**: Provide U235 and Pu239 evaluations
 - **Talou**: Provide new U235 and Pu239 evaluations
 - **Pronyaev**: Provide new U235th based on experimental data
 - **Talou**: Provide script to produce plots experiments vs. given model calculation
 - **Talou/Capote**: write introduction on “Evaluation Methodologies”
 - **Capote**: Collect all **(All)** descriptions of evaluated files to include in final document
1. Evaluation Methodologies: **Capote, Kornilov, Neudecker, Morillon, Shu, Talou, Tudora, Vogt**
 - a. “Only” (differential) experimental data (Cf252sf, U235th)
 - b. Experimental data + model calculations
 - i. Manual tuning of parameters
 - ii. Generalized Least-Squares search of best parameters
 - iii. Monte Carlo sampling of parameters
 - c. Uncertainty Quantification
 - i. Experimental Uncertainties & Correlations
 - ii. Model parameters Uncertainties & Correlations
 - iii. Model limitations
 - d. Description of each ENDF file containing evaluation methodology details (to be given for each ENDF evaluation)
 2. ENDF files available (to be placed on repository- **IAEA**):
 - a. U235th, **Kornilov** (MF5,MT18)
 - b. U235th, **Shu** (MF5, MT18)
 - c. Minsk actinides, **Capote**, 0-20 MeV (MF5,MT18)
 - d. U232-240 (thermal-5.0MeV), **Talou** (MF5,MT18 + MF35,MT18)
 - e. Pu isotopes (thermal-5.0 MeV), **Talou** (MF5,MT18 + MF35,MT18)
 - f. U233,234, (thermal-20MeV), **Tudora** (MF5,MT18)
 - g. Th232, (thermal-20MeV), **Tudora** (MF5,MT18)
 - h. Np237, (thermal-20MeV), **Tudora** (MF5,MT18)
 - i. BRC actinides: U235, U238, Pu239, Pu240 (thermal-20MeV) **Morillon** (MF5,MT18)
 3. To be done within CRP
 - a. Tudora to provide LANL with LA model parameters for U233, U234, Th232, Np237 (1st-chance fission) to compute MF35,MT18 (**Tudora, Neudecker, Talou**)
 - b. Complete U235 and Pu239, all energies (**Talou**)
 - c. U and Pu PFNS evaluations to be re-normalized below 5 MeV (**Talou**)
 - d. Pu239, U235, thermal-20 MeV (**Vogt**)
 4. Summary table & plots
 - a. Average outgoing energies as function of incident energy
 - b. Plots of each evaluation vs. experimental data sets (write script, **Talou, Tudora**)
 - c. Plots of comparisons of evaluations

2.4 Data Testing

ENDF formatted evaluations provided in Nov. 2013 (see Section 4.2 above) to be used for benchmark calculations. Spectrum-average cross section calculations to be performed later on.

Actions:

- **All:** Establish list of benchmarks (see below) & (**Capote**) place on web site
 - **Capote:** Provide updated list of reaction rate values on web site
 - **Capote:** Provide reaction rate calculations
 - **All:** Provide benchmark results from common list to Roberto
 - **All:** Write benchmark testing Section in paper
 - **Capote:** Write SPA Section in paper
 - **Talou:** Provide NUEX data and documentation from Lestone
 - **Talou:** Provide updated NUEX results with updated evaluations
1. Criticality benchmarks, **Kodeli, Morillon, Manturov, Serot**
 - a. Establish list of benchmarks
 2. β -eff benchmarks, **Kodeli**
 - a. Establish list of benchmarks
 3. Reaction rates (IRDFF + revised values) **Capote, Talou (Kahler), Kodeli**
 - a. Establish updated list of reaction rate values for criticality assemblies (CIELO paper), **Capote**
 - b. Perform reaction rate calculations with other evaluated PFNS (thermal, 0.5 MeV, 14 MeV)—no experiments. **Capote**
 4. NUEX data, **Talou (Lestone)**

COMMON AND OPTIONAL BENCHMARK LIST

COMMON BENCHMARK LIST

FAST

Pu-239:

- Jezebel (PU-MET-FAST-001): bare sphere of 95 at.% Pu-239 metal, 4.5 at.% Pu-240, 6.385-cm radius
- Popsy (PU-MET-FAST-006): about 20-cm natural U reflected 94 wt.% Pu-239 sphere, 4.533-cm radius;

U-233:

- Skidoo (U233-MET-FAST-001): bare about 98.1 % U-233 sphere, 5.983-cm radius;
- Flat-top 23 (U233-MET-FAST-006): about 20-cm natural U reflected 98 at.% U-233 sphere, 4.2-cm radius;

U-235:

- Topsy (HEU-MET-FAST-028): about 20-cm natural U reflected 93 wt.% U-235 sphere, 6.116-cm radius;
- Godiva (HEU-MET-FAST-001)

U-238:

- Bigten (IEU-MET-FAST-007): cylinder of 10% enriched U with depleted U-reflector, radius 41.91-cm, height 96.428-cm.

OPTIONAL BENCHMARK LIST

FAST

- ZPPR-9 (ZPPR-LMFR-EXP-002): cylindrical 2-zone, MOX core with Na cooling and depleted U blanket;
- SNEAK-7A and -7B (SNEAK-LMFR-EXP-001): MOX fuel reflected by metallic depleted uranium.

THERMAL

Pu-239:

- PU-SOLUTION-THERMAL-004
- PU-SOLUTION-THERMAL-005

U-235:

- HEU-SOLUTION-THERMAL-001
- HEU-SOLUTION-THERMAL-002

2.5 Open Questions

The following open questions were discussed during the meeting but no recommendations were reached. Some of them may be addressed in the planned technical paper.

- Cf252sf: need for new measurements? Valid at all outgoing energies? Relevance to other isotope measurements
- Kornilov, U235, 0.5 MeV: IRMM data not understood yet, no publication available
- Kornilov, Discussion on the model assumptions regarding neutron emission process
- Kornilov, Integral data vs. microscopic data
- Open questions on how to combine experimental data and model calculations, including covariance matrices
- Recommendations for specific new measurements

3. Conclusions

Presentations and discussions during the meeting showed achieved results within the Project. It was noted that all PFNS measurements should be considered as *shape* measurements for evaluation purposes. Much work needs to be done in the next 20 months so that the technical document is finalized. A roadmap and structure of the technical document were extensively reviewed, and responsibilities agreed. A need for a higher energy reference neutron field was also noted.

A publication of the CRP results in the peer-reviewed journal *Nuclear Data Sheets* was agreed just after the meeting concluded. The technical paper documenting the CRP results needs to be submitted by May 2015, and will be published if accepted in January 2016.

Appendix 1. Agenda



3rd Research Coordination Meeting on

Prompt Fission Neutron Spectra of Actinides

IAEA Headquarters, Vienna, Austria
21 – 24 October 2013

Conference Room F0817

AGENDA

Monday, 21 October

- 08:30 - 09:30** **Registration** (IAEA Registration desk, Gate 1)
- 09:30 - 10:00** **Opening Session**
Welcoming address
Introductory Remarks
Election of Chairman and Rapporteur
Adoption of Agenda
- 10:00 - 10:45* *Administrative and Financial Matters related to participants, Coffee break*
- 10:45 - 12:30** **Session 1: Presentations** (max. 30 min. each)
1) Experimental activities and review of available experimental data:
- Vorobyev – U233; Kornilov – U235
- Oberstedt – U238; CEA – Pu239
- Nuclear Data Section – Th232
Data should cover incident neutron energies from thermal up to 20 MeV.
- 12:30 – 14:00* **Lunch**
- 14:00 – 18:00** **Session 1: Presentations** (cont'd)
2) Modelling and evaluation methods:
Kornilov, Tudora, Shu, Serot, Talou, Capote
(Additional contributors – Ohsawa, Schmidt, Morillon)
- Coffee break as needed*

Tuesday, 22 October

09:00 - 12:30 **Session 1: Presentations** (final)
3) Selection of integral benchmarks and data testing:
 Kodeli, Manturov, Capote

Coffee break as needed

12:30 - 14:00 **Lunch**

14:00 – 18:00 **Session 2**
List of outputs, discussion, final timetable

Coffee break as needed

19:00 **Dinner at a restaurant in the city** (see separate information)

Wednesday, 23 October

09:00 - 12:30 **Session 3**
Detailed drafting of the (final) Technical Report and assignment of responsibilities and deadlines.

Coffee break as needed

12:30 - 14:00 **Lunch**

14:00 – 18:00 **Session 3 (cont'd)**
Detailed drafting of the (final) Technical Report and assignment of responsibilities and deadlines.

Coffee break as needed

Thursday, 24 October

09:00 - 12:30 **Session 3 (cont'd)**
Detailed drafting of the (final) Technical Report and assignment of responsibilities and deadlines

Coffee break as needed

12:30 - 14:00 **Lunch**

14:00 – 16:00 **Review of the outputs and report**
Closing of the Meeting

Appendix 2. List of participants



Third Research Coordination Meeting on Prompt Fission Neutron Spectra of Actinides

IAEA Headquarters, Vienna, Austria
21-24 October 2013

LIST OF PARTICIPANTS

CHINA

Yongjing Chen
Department of Physics
China Institute of Atomic Energy (CIAE)
China National Nuclear Corp. (CNNC)
P.O. Box 275-41
Beijing 102413
Tel. +86 10 69 35 84 10
e-mail: cyj@ciae.ac.cn

CHINA

Nengchuan Shu
Department of Physics
China Institute of Atomic Energy (CIAE)
China National Nuclear Corp. (CNNC)
P.O. Box 275-41
Beijing 102413
Tel. +86 10 69 35 84 10
e-mail: nshu2007@gmail.com
nshu@ciae.ac.cn

FRANCE

Benjamin Morillon
Service de Physique Nucleaire
DAM Ile-de-France
Commissariat a l'Energie Atomique
B.P. 12
91680 Bruyeres le Chatel
Tel. +33 1 69 26 57 86
e-mail: benjamin.morillon@cea.fr

USA

Nikolay Kornilov
Accelerator Lab.
Physics and Astronomy Department
Ohio University
Athens, OH 45701
USA
Tel. +1 740 593-0992
e-mail: kornilov@phy.ohiou.edu

ROMANIA

Anabella C. Tudora
Dept of Nuclear Physics
Faculty of Physics
Bucharest University
P.O. Box MG-11
76900 Bucharest-Magurele
Tel. +40 21 4574666
e-mail: anabellatudora@hotmail.com

RUSSIA

Gennady Manturov and Gleb Lomakov
Institute of Physics and Power
Engineering
(IPPE)
Bondarenko Sq. 1
249033 Obninsk, Kaluga Region
Tel. +7 4843994958
e-mail: mant@ippe.ru

USA

Patrick Talou
Group T-2, MS-B283
Theoretical Division
Los Alamos National Laboratory
Los Alamos, NM 87545
Tel. +1 505 665-0993
Fax +1 505 667-1931
e-mail: talou@lanl.gov

USA

Denise Neudecker
Group T-2, MS-B283
Theoretical Division
Los Alamos National Laboratory
Los Alamos, NM 87545
e-mail: dneudecker@lanl.gov

INDIA

Alok Saxena
Trombay
MUMBAI, Maharashtra 400 085
INDIA
Email: aloks@barc.gov.in

INTERNATIONAL ORGANIZATION

Stephan Oberstedt
EC-JRC-IRMM
Neutron Physics Unit
Retieseweg 111
2440 Geel
Belgium
Tel. +32 14 57 1351
e-mail: stephan.oberstedt@ec.europa.eu

RUSSIA

Alexander S. Vorobyev
St. Petersburg Nuclear Physics Institute
(PNPI)
Russian Academy of Sciences
188350 Gatchina
St. Petersburg Oblast
Tel. + 7 8137146444
e-mail:
alexander.vorobyev@pnpi.spb.ru

SLOVENIA

Ivan Kodeli
Institut Jozef Stefan
Jamova 39
1000 Ljubljana
Tel.
e-mail: ivan.kodeli@ijs.si

FRANCE

Olivier Serot
Commissariat a l'Energie Atomique
CEA-Cadarache, Bldg 230
Saint Paul lez Durance F-13108
Tel. +33 44 2257630
e-mail: olivier.serot@cea.fr

IAEA

Nuclear Data Section
Division of Physical and Chemical
Sciences
Vienna International Centre
PO Box 100
1400 Vienna
Fax +43-1-26007

Roberto Capote Noy
Tel. +43-1-2600-21713
e-mail: r.capotenoy@iaea.org

Stanislav Simakov
Tel. +43-1-2600-21717
e-mail: s.simakov@iaea.org

Naohiko Otsuka
Tel. +43-1-2600-21715
e-mail: n.otsuka@iaea.org

Appendix 3. Meeting photo



Appendix 4. Selected reports by meeting participants

1. Total prompt fission neutron spectrum from thermal-neutron-induced fission of ^{235}U

A. S. Vorobyev and O. A. Shcherbakov

Neutron Research Department, Petersburg Nuclear Physics Institute, Gatchina, 188300, Russia

Discussion

The total PFNS of $^{235}\text{U}(n, f)$, $\Phi_U(E_n)$, was obtained. The numerical data are presented in table 1. Because the neutron-energy grid of the recommended total PFNS of $^{252}\text{Cf}(sf)$ is different from the energy grid applied in this experiment, the linear approximation of the recommended one calculated at the points of the energy grid applied in this experiment was used as the standard, $N_{Std}(E_n)$. This linear approximation is also presented in table 1. The total relative errors of the obtained total PFNS, D_Φ , were calculated assuming that all errors mentioned above are independent and that the distribution of systematic errors is uniform:

$$D_\Phi^2 = D_U^2 + D_{Cf}^2 + \frac{(D_{Bckg}^2 + D_{BW}^2 + D_{En}^2)}{3} + D_{Std}^2 \quad (27)$$

where D_U and D_{Cf} are the relative errors on the total PFNS measurement obtained from eq. (23) for $^{235}\text{U}(n, f)$ and $^{252}\text{Cf}(sf)$, respectively; D_{Std} is the relative accuracy of the $^{252}\text{Cf}(sf)$ standard $N_{Std}(E_n)$ [3]; D_{Bckg} is the maximum relative uncertainty of the ratio $R(E_n)$ caused by the systematic uncertainty in the background determination; $D_{BW}(E_n)$ is the relative accuracy of the bin-width correction $B(E_n)$; and D_{En} is the maximum relative uncertainty of the ratio $R(E_n)$ arising from the neutron-energy-grid uncertainty, considering the fact that the neutron-detector length is 8% of the time-of-flight basis.

As mentioned previously, a linear approximation was used to estimate the background contribution remaining in the measured neutron time-of-flight spectra after the subtraction of all known components of the background. Two versions of the data processing with different

approximation parameters $R^*(E_n)$ were performed. The following equation was used to determine the corresponding systematic error:

$$D_{Bckg}(E_n) = \max \left(\left| \frac{R^*(E_n) - R(E_n)}{R(E_n)} \right| \right) \quad (28)$$

To determine the maximum uncertainty D_{En} , the ratio of the total PFNS of $^{235}\text{U}(n, f)$ to the total PFNS of $^{252}\text{Cf}(sf)$ was obtained for two time-of-flight bases $D^+ = d + h/2 + \delta h$ and $D^- = d - h/2 - \delta h$. The obtained ratios $R^+(E_n)$ and $R^-(E_n)$ are presented in fig. 12. The corresponding systematic error of the ratio $R(E_n)$ was determined using the following expression:

$$D_{En}(E_n) = \frac{|R^+(E_n) - R(E_n)| + |R^-(E_n) - R(E_n)|}{2R(E_n)} \quad (29)$$

To demonstrate the difference from the Maxwell distribution frequently used for the description of the total PFNS, fig. 13 presents the ratio of the total PFNS of $^{235}\text{U}(n, f)$ to a Maxwell distribution with parameters $\nu_U = 2.421$ (ENDF/B-VII) and $T_M = 1.314$ MeV [8]:

$$\mu(E_n) = \frac{\Phi_U(E_n)}{M(T_M, E_n)\nu_U} = \frac{R(E_n)N_{Std}(E_n)\nu_{Cf}}{M(T_M, E_n)\nu_U} \quad (30)$$

The experimental data from refs. [8–10] and the ENDF/B-VII evaluation [3] are also shown for comparison. All experimental spectra shown in this figure were measured using the time-of-flight method and obtained from the total PFNS of $^{235}\text{U}(n, f)$ measured relative to that of $^{252}\text{Cf}(sf)$ using eq. (30). In ref. [8], different neutron detectors were used for different neutron-energy ranges: 1) 0.08 - 0.9 MeV – anthracene crystal coupled to PMT-71 (time-of-flight basis of 51 cm); 2) 1 - 8 MeV – stilbene crystal coupled to PMT-63 (time-of-flight basis of 231.3 cm); and 3) 4 - 12 MeV – plastic scintillator coupled to PMT-63 (time-of-flight basis of 611 cm). To investigate the total PFNS in the energy range of 0.03 to 4 MeV [9], lithium glass (NE-912) coupled to PMT-30 was applied for neutron detection at a 30-cm time-of-flight basis. The data in ref. [10] covered a wide neutron-energy range (from 0.7 to 12 MeV) and were obtained using detectors manufactured by SCIONIX, which consisted of NE-213-equivalent scintillator LS301 coupled to PMT XP4312; the detectors were located at a time-of-flight basis of approximately 300 cm.

The given representation of the existing total PFNS data allows the estimation of the

confidence level of the obtained data and the identification of possible systematic errors inherent to the experimental method followed. Because the detection efficiency of the fission fragments $N_f(\theta)$ for the given data is known with an accuracy of approximately 1 - 2%, an additional normalization was applied (fig. 14) to exclude this uncertainty from the data presented in fig. 13:

$$\mu'(E_n) = \mu(E_n)K_N \quad K_N = \frac{\nu_U}{\nu_{fit}} \quad (31)$$

where K_N and ν_{fit} are the normalization coefficient and the average total number of prompt neutrons per fission event of $^{235}\text{U}(n, f)$, respectively, obtained by fitting the experimental data. It is well known [11] that the Watt distribution W given by eq. (32) can be used to describe the total PFNS as an alternative to the Maxwellian description, eq. (24):

$$W = \nu_{fit} \sqrt{\pi E_W T_W} \exp\left(-\frac{E_W + E_n}{T_W}\right) \sinh\left(\frac{2\sqrt{E_W E_n}}{T_W}\right) \quad (32)$$

The average energy of a Watt distribution with parameters E_W and T_W is $\langle E_n \rangle = E_W + 3T_W / 2$. Therefore, fitting the total PFNS experimental data with a Watt distribution provides a better description across a wide neutron-energy range. The total PFNS data shown in fig. 13 were fitted with a Watt distribution, eq. (32), in the neutron-energy range from 1 to 10 MeV. The results of this fit are given in table. 2. For comparison, a fit performed with a Maxwell distribution is also presented. The data [8] obtained from two different experimental set-ups agree within the errors in the neutron-energy range from 4 to 8 MeV, and furthermore, they are consistent with being the same data set (fig. 13). The adjusted normalization coefficient K_N for a Watt distribution within the accuracy of the experimental data is close to 1, while for the Maxwell distribution, the deviation from 1 exceeds the accuracy of the detection efficiency of the fission fragments. This observation provides an additional argument for the use of the Watt distribution as the interpolation function for the determination of the normalization coefficient K_N given by eq. (31).

As can be observed in fig. 14, all of the experimental data are in agreement within the experimental errors on the observed shape of the total PFNS in the neutron-energy range from 1 to 10 MeV (approximately 70% of the total number of neutrons fall within this energy range). The reference data shown in fig. 14, excluding the data of ref. [8], could also be

described by the ENDF/B-VII evaluation performed under the assumption that the prompt fission neutrons are evaporated by fully accelerated fragments. In this case, the normalization coefficient K_N adjusted to the data of ref. [8] is equal to 1.045, which is outside the given experimental error.

In the low-neutron-energy range from 0.1 to 1 MeV (fig. 15), the uncertainties of the data increase. This increased uncertainty is most likely related to some ambiguity in accounting for the neutron detector background. The situation becomes more complicated because in the analysis of the data of refs. [8, 9], it is not possible to disregard the normalization uncertainty analogous to that existing in the neutron-energy range above 1 MeV. Therefore, new time-of-flight experiments performed by different research groups and using various detectors for neutron detection are requested to define the total PFNS in the low-neutron-energy range.

To summarize, the most accurate description of the experimental data has been obtained using a Watt distribution. Some differences between the total evaluated PFNS shape (ENDF/B-VII) and the experimental one are related to both the experimental difficulties inherent in the spectrum measurement and the limitations of the model used for the evaluation. Most likely, the statistical model evaluation of the total PFN spectrum should account for the neutron emission anisotropy caused by the presence of the fragment angular momentum and the possibility of the existence of neutrons emitted either by incompletely accelerated fragments or during the initial stage of the fission process (the so-called “scission” neutrons) [12]. In contrast to the works presented in figs. 13, 14 and 15, in the present research, the total PFNS was obtained by the numerical integration of the partial PFNS measured at fixed angles with respect to the fission axis. Because agreement within the experimental errors is observed among the data obtained by different methods, it is possible to conclude that the contribution of the “scission” neutrons to the total PFNS is comparatively small.

References

1. A.S. Vorobyev, O.A. Shcherbakov, Yu.S. Pleva *et.al.*, Nucl. Instrum. Methods A **598**, 795 (2009).
2. A.S. Vorobyev, O.A. Shcherbakov, Yu.S. Pleva *et.al.*, *Neutron Spectroscopy, Nuclear*

Structure, Related Topics, in Proceedings of the XVII International Seminar on Interaction of Neutrons with Nuclei, ISINN-17, 27-29 May 2009, JINR, Dubna, Russia, edited by A.M. Sukhovoij, JINR, **E3-2010-36**, 60 (2010).

3. C.W. Reich, W. Mannhart, T. England, ENDF/B-VII.

4. E.A. Seregina, P.P. Dyachenko, VANT, Ser.: Nuclear Constants, v.1, 58 (1985), *in Russian*.

5. H.R. Bowman, S.G. Thompson, J.C.D. Milton, W.J. Swiatecki, Phys. Rev. **126**, 2120 (1962).

6. W.P. Poenitz, T. Tamura, *Nuclear Data for Science and Technology, in Proceedings of the International Conference, 6-10 September 1982, Antwerp, Belgium*, edited by K.H. Bockhoff, 465 (1983).

7. E.A. Seregina, P.P. Dyachenko, Sov. J. Nucl. Phys. **42**, n. 6(12), 1337 (1985), *in Russian*.

8. V.N. Nefedov, B.I. Starostov, A.A. Boitsov, *Neutron Physics, in Proceedings of 6-th All-Union Conference, 2-6 October 1983, Kiev, USSR.. Moscow, Part 2*, 285 (1984). VANT, Ser.: Nuclear Constants, v.3, 16 (1985), *in Russian*. EXFOR 40871011, 40871012, 40872007.

9. A. Lajtai, J. Kecskemeti, J. Safar *et. al.*, IAEA-TECDOC-335, 312 (1985), EXFOR 3070403.

10. N. Kornilov, F.-J. Hamsch, I. Fabry *et. al.*, Nucl. Sci. and Eng. **165**, 117 (2010).

11. J. Terrell, Phys. Rev. **113**, 527 (1959).

12. A.S. Vorobyev, O.A. Shcherbakov, A.M. Gagarski *et.al*, EPJ Web of Conference **8**, 03004 (2010). DOI: 10.1051/epjconf/20100803004.

Table 1. Total PFNS of $^{235}\text{U}(n, f)$.

E_n , MeV	$R(E_n)$	D_R	D_U	D_{Cf}	D_{Bckg}	D_{BW}	D_{En}	$N_{Std}(E_n)$ 1/MeV $\times 10^4$	D_{Std}	$\Phi_U(E_n)$ Neutr/MeV $\times 10^4$	D_ϕ
16.650	0.1577	0.469	0.367	0.142	0.231	0.027	0.376	0.1812	0.156	0.1074	0.494
13.290	0.2961	0.259	0.143	0.107	0.156	0.023	0.284	1.759	0.045	1.958	0.263
10.860	0.3880	0.167	0.068	0.076	0.059	0.019	0.221	9.103	0.029	13.3	0.170
9.043	0.4299	0.127	0.038	0.062	0.027	0.016	0.177	30.7	0.022	49.6	0.129
7.647	0.4778	0.098	0.031	0.041	0.015	0.013	0.143	77.9	0.019	139.9	0.100
6.552	0.5403	0.079	0.024	0.032	0.010	0.010	0.118	160.8	0.016	326.6	0.081
5.677	0.5651	0.067	0.016	0.031	0.007	0.009	0.098	283.6	0.015	602.4	0.068
4.967	0.5912	0.054	0.015	0.021	0.004	0.007	0.082	444.5	0.014	987.8	0.056
4.383	0.6169	0.046	0.013	0.019	0.003	0.006	0.069	640.0	0.013	1484.2	0.048
3.896	0.6266	0.039	0.011	0.017	0.002	0.005	0.058	859.1	0.012	2023.6	0.041
3.486	0.6449	0.033	0.010	0.014	0.002	0.004	0.049	1092	0.012	2647.1	0.035
3.137	0.6494	0.031	0.009	0.016	0.001	0.004	0.042	1331	0.012	3249.0	0.033
2.839	0.6437	0.026	0.008	0.015	0.001	0.003	0.035	1564	0.012	3784.3	0.029
2.581	0.6552	0.023	0.007	0.014	0.001	0.003	0.030	1785	0.012	4396.4	0.026
2.357	0.6784	0.022	0.007	0.015	0.001	0.002	0.025	1994	0.011	5084.7	0.024
2.161	0.6632	0.019	0.008	0.012	0.001	0.002	0.021	2187	0.011	5452.3	0.021
1.988	0.6782	0.018	0.008	0.013	0.001	0.002	0.017	2365	0.012	6028.9	0.022
1.835	0.6761	0.017	0.008	0.012	0.001	0.002	0.014	2524	0.012	6415.1	0.020
1.699	0.6744	0.015	0.007	0.011	0.001	0.002	0.011	2671	0.013	6770.6	0.020
1.578	0.6616	0.018	0.008	0.015	0.001	0.001	0.009	2792	0.012	6943.5	0.021
1.469	0.6646	0.017	0.008	0.015	0.001	0.001	0.007	2900	0.012	7245.3	0.021
1.372	0.6765	0.019	0.007	0.017	0.001	0.001	0.005	2995	0.012	7615.8	0.022
1.283	0.6735	0.014	0.009	0.010	0.001	0.001	0.003	3075	0.012	7784.4	0.018
1.203	0.6686	0.016	0.008	0.014	0.001	0.001	0.002	3147	0.012	7909.7	0.020
1.130	0.6817	0.014	0.009	0.011	0.001	0.001	0.001	3199	0.012	8197.6	0.019
1.064	0.6763	0.019	0.009	0.017	0.001	0.001	0.001	3243	0.013	8244.2	0.023
1.003	0.6746	0.021	0.009	0.019	0.001	0.001	0.001	3283	0.016	8325.0	0.026
0.948	0.6776	0.017	0.009	0.014	0.001	0.001	0.001	3311	0.017	8432.8	0.024
0.896	0.6668	0.024	0.011	0.021	0.001	0.001	0.001	3333	0.018	8354.2	0.030
0.849	0.6681	0.019	0.010	0.016	0.001	0.001	0.001	3352	0.018	8418.5	0.026
0.806	0.6648	0.024	0.011	0.021	0.001	0.001	0.001	3360	0.018	8396.8	0.030
0.766	0.6756	0.025	0.011	0.022	0.001	0.001	0.002	3360	0.018	8533.3	0.031
0.728	0.6717	0.021	0.013	0.017	0.001	0.001	0.003	3360	0.019	8483.7	0.029
0.694	0.6623	0.025	0.011	0.022	0.001	0.000	0.004	3360	0.018	8365.1	0.031
0.661	0.6720	0.026	0.013	0.022	0.001	0.000	0.006	3353	0.017	8469.8	0.031
0.631	0.6597	0.023	0.013	0.019	0.001	0.000	0.008	3341	0.016	8285.0	0.028
0.603	0.6660	0.028	0.015	0.023	0.001	0.000	0.010	3329	0.017	8335.0	0.033
0.577	0.6782	0.029	0.014	0.024	0.002	0.000	0.012	3318	0.018	8458.3	0.034
0.553	0.6602	0.030	0.015	0.025	0.002	0.000	0.015	3298	0.018	8184.7	0.035
0.530	0.6666	0.032	0.015	0.027	0.002	0.000	0.017	3280	0.018	8218.7	0.037
0.488	0.6853	0.022	0.010	0.015	0.002	0.000	0.023	3229	0.017	8318.2	0.028
0.434	0.6671	0.027	0.010	0.016	0.002	0.001	0.033	3164	0.017	7933.9	0.032
0.388	0.6411	0.035	0.011	0.022	0.002	0.000	0.044	3076	0.017	7423.1	0.039
0.349	0.7089	0.044	0.014	0.027	0.003	0.001	0.055	2998	0.017	7988.8	0.047
0.316	0.6603	0.047	0.015	0.021	0.003	0.000	0.067	2921	0.017	7249.8	0.050
0.287	0.6681	0.057	0.019	0.029	0.003	0.000	0.079	2840	0.018	7132.0	0.060
0.263	0.6328	0.068	0.022	0.037	0.003	0.000	0.090	2755	0.018	6553.5	0.070
0.241	0.6919	0.077	0.028	0.042	0.007	0.000	0.101	2675	0.019	6957.0	0.080
0.221	0.6824	0.097	0.036	0.059	0.029	0.000	0.113	2598	0.021	6664.2	0.099

Table 2. Fitting parameters of the total PFNS of ^{235}U . The given errors are the mean square-root deviations of the experimental data from the distribution used to fit the experimental data.

Watt distribution, eq. (32)					
Reference	T_W , MeV	E_W , MeV	$\langle E_n \rangle$, MeV	v_{fit}	K_N
Present work	0.954 ± 0.033	0.592 ± 0.041	2.023 ± 0.012	2.440 ± 0.014	0.992
[8]	0.983 ± 0.031	0.521 ± 0.041	1.995 ± 0.011	2.353 ± 0.011	1.029
[10]	0.968 ± 0.006	0.534 ± 0.008	1.985 ± 0.003	2.461 ± 0.002	0.984
Maxwell distribution, eq. (24)					
	T_M , MeV	$\langle E_n \rangle$, MeV	v_{fit}	K_N	
Present work	1.390 ± 0.009	2.089 ± 0.014	2.509 ± 0.010	0.965	
[8]	1.353 ± 0.006	2.030 ± 0.009	2.404 ± 0.006	1.007	
[10]	1.339 ± 0.003	2.009 ± 0.004	2.513 ± 0.004	0.963	

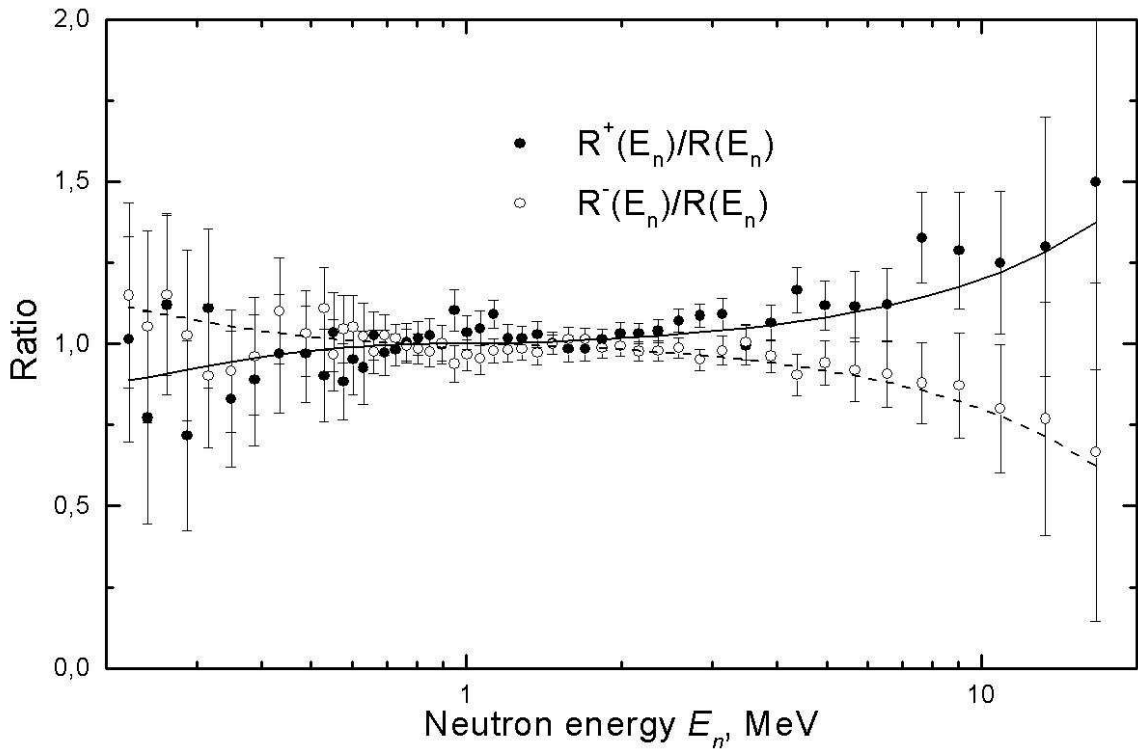


Fig. 12. Ratio of the total PFNS of $^{235}\text{U}(n, f)$ to the total PFNS of $^{252}\text{Cf}(sf)$ obtained for two flight paths defined as the distance between the fissile target and the front (open circles) or rear (full circles) surface of the stilbene crystal.

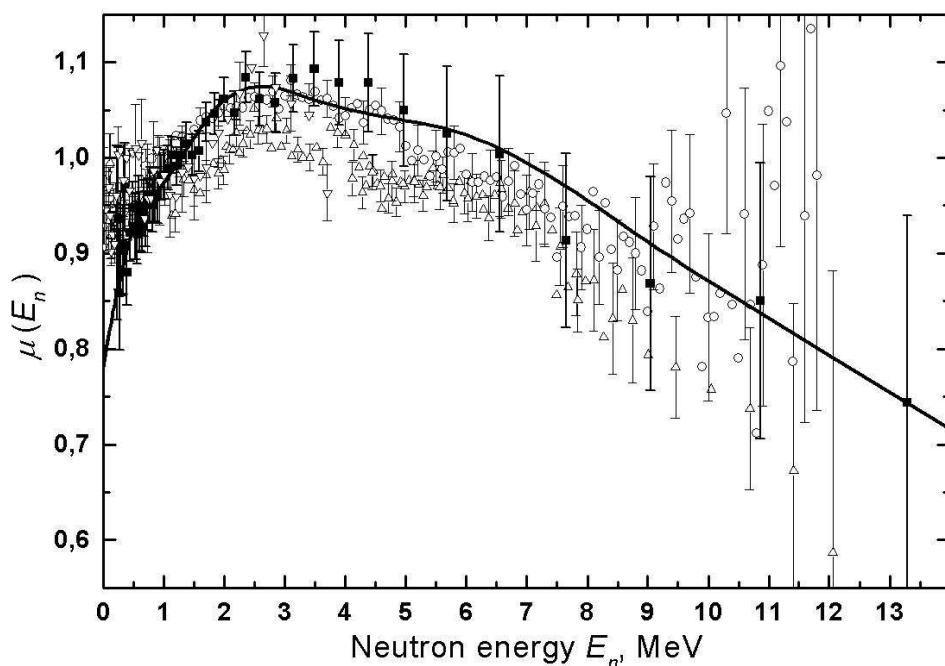


Fig. 13. Ratio of the total PFNS of $^{235}\text{U}(n, f)$ to the Maxwell distribution of eq. (24) with $T_M = 1.314$ MeV: full square - present work; circle - [10]; upward triangle - [8]; downward triangle - [9]; and thick line - evaluation ENDF/B-VII.

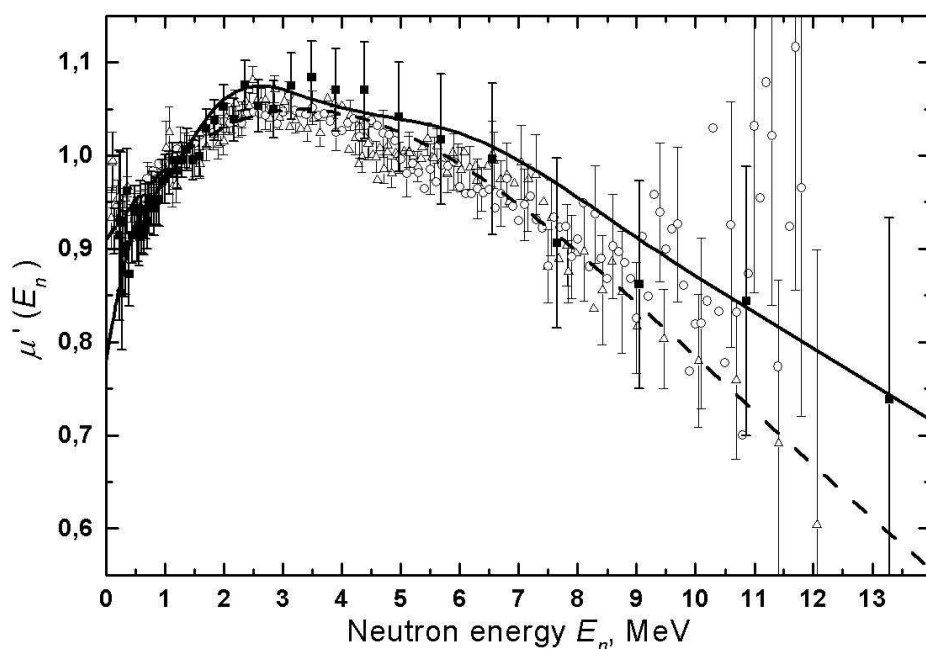


Fig. 14. Ratio of the total PFNS of $^{235}\text{U}(n, f)$ normalized according to eq. (31) to the Maxwell distribution of eq. (24) with $T_M = 1.314$ MeV: full square - present work; circle - [10]; upward triangle - [8]; downward triangle - [9]; thick line - evaluation ENDF/B-VII; and thin

line - Watt distribution of eq. (32) with parameters from [8]. The energy scale is linear.

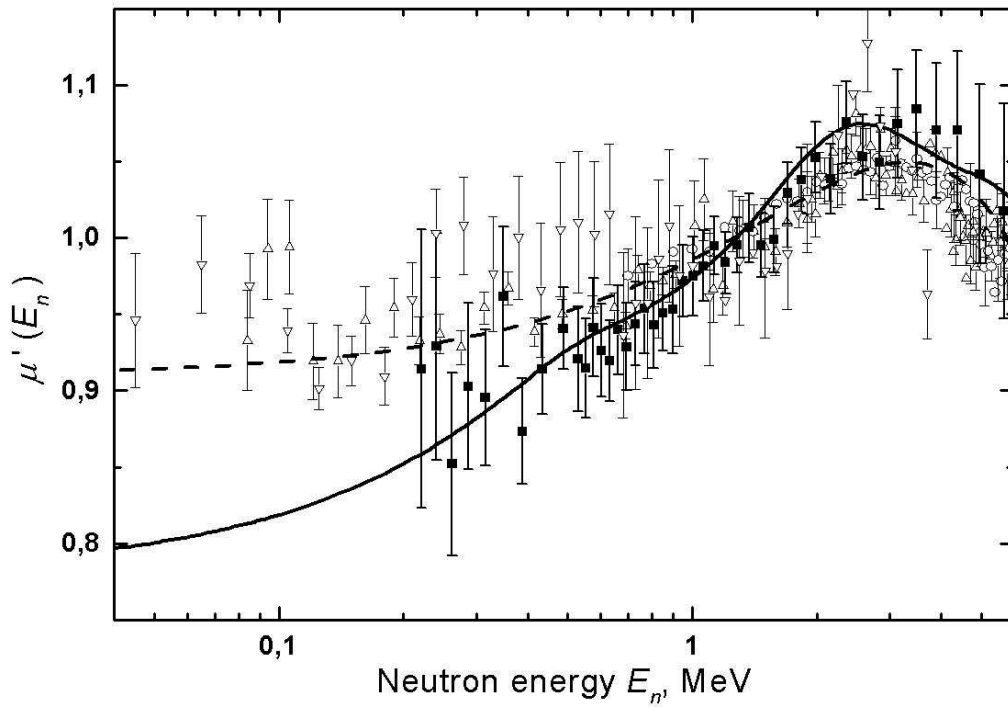


Fig. 15. Ratio of the total PFNS of $^{235}\text{U}(n, f)$ normalized according to eq. (31) to the Maxwell distribution of eq. (24) with $T_M = 1.314$ MeV: full square - present work; circle - [10]; upward triangle - [8]; downward triangle - [9]; thick line - evaluation ENDF/B-VII; and thin line - Watt distribution (32) with parameters from [8]. The energy scale is logarithmic.

2. Model calculations of prompt fission neutron spectra of $^{232}\text{Th}(n,f)$

Anabella Tudora, University of Bucharest, Faculty of Physics

1. Introduction

With increasing awareness of the global changes of the environment, nuclear power is regaining its position as the most appropriate option to produce great quantities of energy with negligible emission of greenhouse gases. This position is subject to the conditions of increased safety, reduction of the risk of fissile material proliferation and a viable solution to the problem of long-term radioactive waste disposal.

In this context new concepts of nuclear technology for power production are being investigated, the thorium-based nuclear fuel cycle being an appropriate option because of advantages such as: *i*) the fissile nucleus ^{233}U of this fuel cycle is a very efficient nuclear fuel (a reactor concept based on Th-U fuel being feasible); *ii*) the world reserves of Th are much larger than the reserves of uranium; *iii*) the production of long-live actinides, which are the main source of long-term residual radioactivity of the nuclear waste, is much smaller in the Th-U fuel. This fact can be used with advantage in the design of critical as well as sub-critical accelerator-driven systems (ADS); *iv*) the Th-U fuel is more proliferation-resistant due to the highly radioactive constituents which cannot be separated out by chemical means. Handling of such materials in improvised clandestine laboratories is practically impossible [1].

Because of the previous lack of interest concerning the Th-fuel cycle, the quality of nuclear data for the relevant materials was and remains lower than for comparable materials in the uranium or mixed U-Pu oxide (MOX) fuel cycle. For this reason numerous activities are in progress in many countries in order to make possible the use of the thorium-based fuel for ADS applicable to power production and radioactive waste transmutation.

The evaluation of nuclear data for relevant actinides of the Th-U fuel cycle is an important requirement. To answer these needs in the last decade new measurements of neutron-induced fission cross-sections of light actinides were performed (i.e. fission cross-sections of ^{233}Pa , ^{231}Pa and ^{233}U in the fast neutron energy range). A large effort to provide accurate evaluated data for light actinides (especially neutron induced cross-sections) was made particularly in the framework of an IAEA coordinated research programme devoted to the Th-U cycle [2].

Besides the experimental and evaluation efforts mentioned above, experimental prompt emission data of light actinides are generally scarce or almost missing for certain isotopes. Much more accurate evaluations of their prompt emission data are necessary, too. To answer these needs, an IAEA coordinate research programme concerning the prompt fission neutron spectra of actinides is in progress [3].

For the basic fertile nucleus ^{232}Th of the Th-U cycle, the present status of prompt emission data can be synthesized as following.

Experimental prompt emission data of $^{232}\text{Th}(n,f)$ exist only for the following total average quantities:

- total average prompt neutron multiplicity $\langle v_p \rangle_{\text{tot}}$ as a function of incident neutron energy (E_n) (the data sets of EXFOR [4] covering the E_n range from 1.3 MeV up to above 20 MeV),

- total average prompt neutron spectra (PFNS) (spectrum data available in EXFOR [5] are measured at a few En values i.e. 2 MeV, 2.9 MeV, 14.6 MeV, 17.7 MeV) and
- total average prompt gamma-ray energy $\langle E_\gamma \rangle_{\text{tot}}$ as a function of En, an unique data set measured by Fréhaut [6] (with En ranging from 2.35 MeV up to about 15 MeV).

Experimental prompt emission data as a function of fragment mass number (A) or as a function of total kinetic energy (TKE) are completely missing for ^{232}Th .

In recent evaluated nuclear data libraries the status of prompt emission data is the following: $\langle v_p \rangle_{\text{tot}}$ of JENDL4 [7] is a linear function fit to the experimental data and the PFNS are provided by the CCONE code. Total average prompt multiplicity and spectra of JEFF3.1.2 [8] are the results of a semi-empirical emissive model (see details in Ref.[9] and references therein). In ENDF/B-VII [10] the $\langle v_p \rangle_{\text{tot}}$ calculation was renormalized to the evaluation based on experimental data.

Taking into account the important role of ^{232}Th in the Th-U fuel cycle, the practical purpose of the present work is to provide an improved evaluation of prompt emission data. A consistent model calculation of prompt neutron and gamma-ray data of ^{232}Th is proposed.

The Point-by-Point model (PbP) of prompt emission, already successfully used to provide all prompt emission quantities of many actinides (see for instance Refs. [11-13] and references therein) is applied for the first time to $^{232}\text{Th}(n,f)$. The $\bar{\nu}(A)$ behaviour consisting in the multiplicity increase with En for heavy fragments only (observed experimentally in the case of $^{235}\text{U}(n,f)$ at 0.5 and 5.5 MeV and $^{237}\text{Np}(n,f)$ at 0.8 and 5.5 MeV and confirmed by model calculations) is obtained in the case of $^{232}\text{Th}(n,f)$ as well.

The correlation between the sub-barrier resonant behaviour of the fission cross-section of fertile actinides (characterizing the pre-scission stage) and the fluctuations of their fission fragment and prompt emission data (characterizing the post-scission stage), already discussed for two fertile nuclei $^{234}\text{U}(n,f)$ [12] and $^{238}\text{U}(n,f)$ [13] is supported by the case of $^{232}\text{Th}(n,f)$, too.

The prompt emission model calculation is validated by the very good description of experimental $\langle v_p \rangle_{\text{tot}}$ and $\langle E_\gamma \rangle_{\text{tot}}$ over the entire fast neutron energy range. PFNS obtained in a consistent way (meaning concomitantly in the same run and without any adjustments) also describe well the existing experimental data.

2. Brief mention of prompt emission models used

The basic features of the PbP model were described in many previous papers (see for instance the appendix of Ref. [11] and references therein).

In the present PbP calculations the fragmentation range was constructed by taking all fragment mass pairs from symmetric fission up to the far asymmetric split $A_H=159$, $A_L=74$. For each mass pair three fragments were taken with the charge numbers Z as the nearest integers above and below the most probable charge. The mass excesses needed in PbP calculations were taken from the database of Audi and Wapstra [14], the shell corrections entering the generalized super-fluid model used to provide the level density parameters of fragments are taken from the database of Möller and Nix [15]. The compound nucleus cross-sections of the inverse process of neutron evaporation from fragments $\sigma_c(\epsilon)$ are provided by

optical model calculations (using the latest version of the code SCAT2) [16] with phenomenological potentials appropriate for nuclei appearing as fission fragments (e.g. Becchetti-Greenlees, Koning-Delaroche taken from [17]). The total excitation energy partition based on modeling at scission (described in [11, 18]) is used in this case, too.

To obtain average quantities characterizing the fragments and the prompt neutron and gamma-ray emission the multi-parametric matrices provided by the PbP model are averaged over different fragment distributions as described in Refs. [11, 12]. The charge distribution of each fragment pair of the fragmentation range is taken as a narrow Gaussian (according to Ref. [19]).

In the case of $^{232}\text{Th}(n,f)$ experimental fragment mass and total kinetic energy distributions ($Y(A)$ and $\text{TKE}(A)$) exist in the EXFOR library at six incident neutron energies: 1.6 MeV, 1.75 MeV, 2 MeV, 2.5 MeV, 3 MeV and 5.8 MeV [20]. These experimental fragment distributions give the possibility to apply the PbP model to provide different quantities of prompt neutron and gamma-ray emission as a function of fragment mass and of E_n .

At higher incident neutron energies, where multiple fission chances are involved, total average prompt emission quantities (e.g. $\langle v_p \rangle_{\text{tot}}$, $\langle E_\gamma \rangle_{\text{tot}}$, PFNS) are calculated in the frame of the most probable fragmentation approach (Los Alamos model of Madland and Nix [21] with subsequent improvements as mentioned in [11] and references therein) using average model parameters depending on excitation energy. These parameters are obtained from the PbP treatment in the case of the main fissioning nucleus ^{233}Th and from systematics [22] in the case of secondary fissioning nuclei $^{232-230}\text{Th}$. The fission cross-section ratios (expressing the fission probability of each compound nucleus) required by the most probable fragmentation approach are taken from recent evaluations [23, 24].

In the PFNS calculation at high E_n the spectra of neutrons emitted prior to the fission are provided by nuclear reaction calculations using an improved version of the GNASH code. All parameters required in calculations (i.e. fission barrier parameters, level densities and so on) are taken from Ref. [25]. This work provided an excellent description of sub-barrier resonances in the fission cross-section of the ^{232}Th due to the refined fission model with sub-barrier effects developed by Vladuca et al. (see for instance [26, 27] and references therein) extended for triple-humped barriers in the discrete part of transition state spectrum as described in Ref. [25].

3. Results and discussions

3.1 PbP calculations of prompt emission related data as a function of fragment mass

The prompt emission quantities as a function of fragment mass, especially the average prompt neutron multiplicity $\bar{\nu}(A)$, are very sensitive to the partition of total excitation energy (TXE) between complementary fully-accelerated fission fragments. The comparison of $\bar{\nu}(A)$ with experimental data -when they exist- being a crucial test of the TXE partition. Unfortunately, in the case of $^{232}\text{Th}(n,f)$ experimental data as a function of fragment mass are completely missing.

In the present PbP calculation the TXE partition based on the modeling at scission (described in [11, 18]) was used. This method was already successfully applied for other fissioning

systems, leading to PbP results of $\bar{\nu}(A)$ and $\bar{E}_\gamma(A)$ describing well the experimental data. This is the case of $^{252}\text{Cf}(\text{SF})$, $^{235}\text{U}(\text{n,f})$, $^{237}\text{Np}(\text{n,f})$, $^{239}\text{Pu}(\text{n}_{\text{th}},\text{f})$, $^{233}\text{U}(\text{n}_{\text{th}},\text{f})$ (details can be found in [12, 13, 18, 28, 29] and references therein).

An example of excitation energies at full acceleration resulted from the modeling at scission is given in **Fig.1** where $E^*(A)$ calculated at $E_n = 2$ MeV (open squares), 2.9 MeV (full circles) and 5.8 MeV (stars) are given. An increase of $E^*(A)$ with E_n is observed mainly for the heavy fragments, suggesting the $\bar{\nu}(A)$ behaviour observed experimentally in the case of $^{235}\text{U}(\text{n,f})$ at 0.5 MeV and 5.55 MeV [30] and $^{237}\text{Np}(\text{n,f})$ at 0.8 MeV and 5.5 MeV [31].

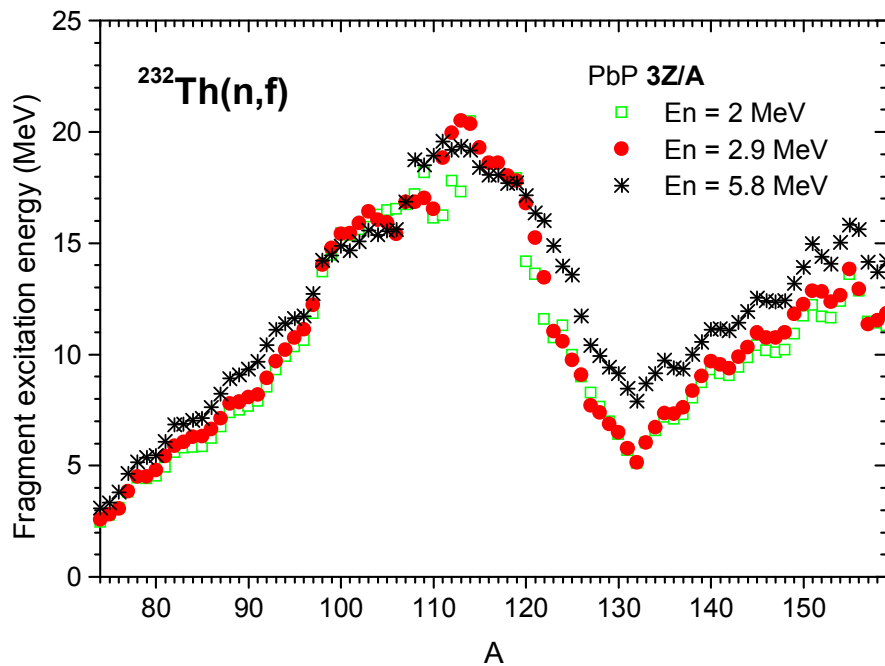


Fig.1 Fragment excitation energy as a function of fragment mass number $E^*(A)$ at $E_n = 2$ MeV (open squares), 2.9 MeV (full circles) and 5.8 MeV (stars).

Prompt emission calculations done for many fissioning systems using very different TXE partitions in the frame of different approaches (the present deterministic PbP model and the probabilistic Monte-Carlo treatment [32]) revealed *the insensibility of the prompt neutron multiplicity of fragment pair $\nu_{\text{pair}} = \nu_L + \nu_H$ to the TXE partition* (for details see [12] and references therein).

This finding is very important taking into account that the TXE partition is not yet completely elucidated, several methods based on different physical assumptions being proposed and used in prompt emission calculations (see for instance [18, 32, 33, 34]).

Consequently even if the TXE partition based on modeling at scission used in the present calculation is not the most appropriate one, the insensitivity of ν_{pair} to the TXE partition leads to a trustful prediction of average prompt emission data of ^{232}Th .

PbP results of $\bar{\nu}_{\text{pair}}(A_H)$ at incident energies ranging from 1.6 MeV to 5.8 MeV are given in **Fig.2**. As observation, the fragmentation range being constructed by taking three charge numbers Z for each mass number A , $\bar{\nu}_{\text{pair}}$ plotted in Fig.2 as a function of A_H as well as all

quantities given as a function of A were obtained by averaging over the charge distribution.

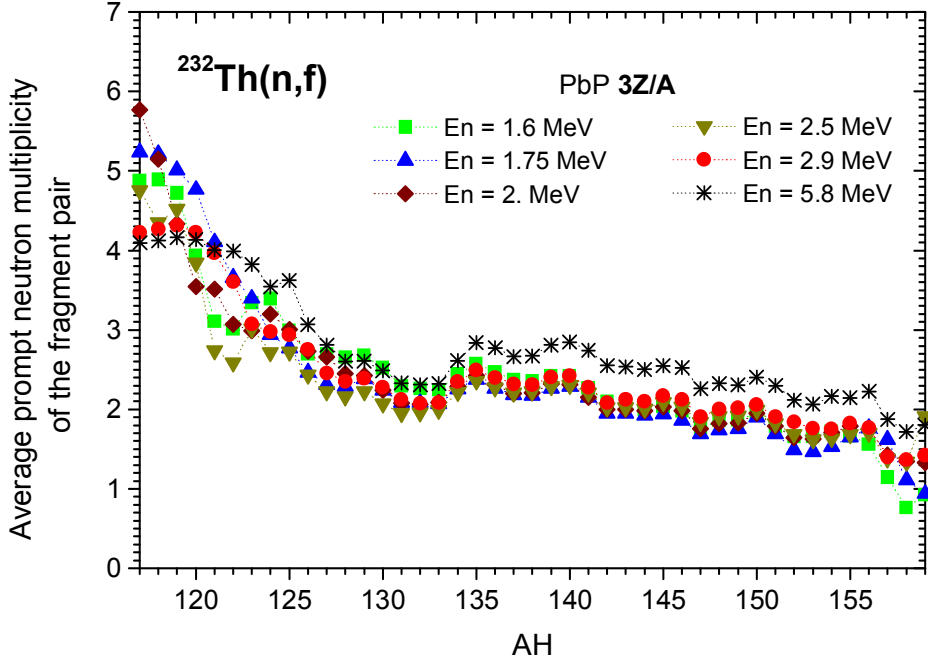


Fig.2: PbP results of prompt neutron multiplicity of fragment pairs as a function of heavy fragment mass number A_H at six incident neutron energies ranging from 1.6 MeV to 5.8 MeV.

Examples of $\bar{\nu}(A)$ calculations are plotted in **Fig.3** with red circles at $E_n = 2.9$ MeV and black stars at $E_n = 5.8$ MeV. The multiplicity increase with E_n for mainly heavy fragments (observed experimentally in the case of ^{235}U and ^{237}Np and confirmed by PbP model calculations for these fissioning systems and for others, too, see [12, 18] and references therein) is visible in the case of ^{232}Th , too.

Average prompt gamma-ray energy as a function of fragment mass $\bar{E}_\gamma(A)$ at $E_n = 2.9$ MeV and 5.8 MeV are plotted in **Fig.4** with the same symbols and colors as in Fig.3. As it can be seen in Fig.4 the $\bar{E}_\gamma(A)$ results also exhibit a sawtooth shape, but the behaviour with E_n does not reveal the \bar{E}_γ increase for heavy fragments only.

The average prompt gamma multiplicity of fragment pairs $\langle N_\gamma \rangle_{\text{pair}}$ can be calculated by using the experimental variance σ_γ^2 measured by Fréhaut that is given as a linear fit to the average prompt neutron multiplicity in Ref. [6]. The results of $\langle N_\gamma \rangle_{\text{pair}}$ as a function of A_H are plotted in the upper part of **Fig.5** with green squares ($E_n = 2$ MeV), red circles ($E_n = 2.9$ MeV) and black stars ($E_n = 5.8$ MeV). Contrary to the prompt neutron multiplicity $\bar{\nu}_{\text{pair}}(A_H)$ showing an increase with the incident energy (see Fig.2) the average prompt gamma multiplicity of fragment pairs $\langle N_\gamma \rangle_{\text{pair}}$ remains almost constant. This result is in agreement with the observation of Fréhaut [6] concerning the total average number of prompt gamma quanta derived from experimental data that remains almost constant with the incident neutron energy.

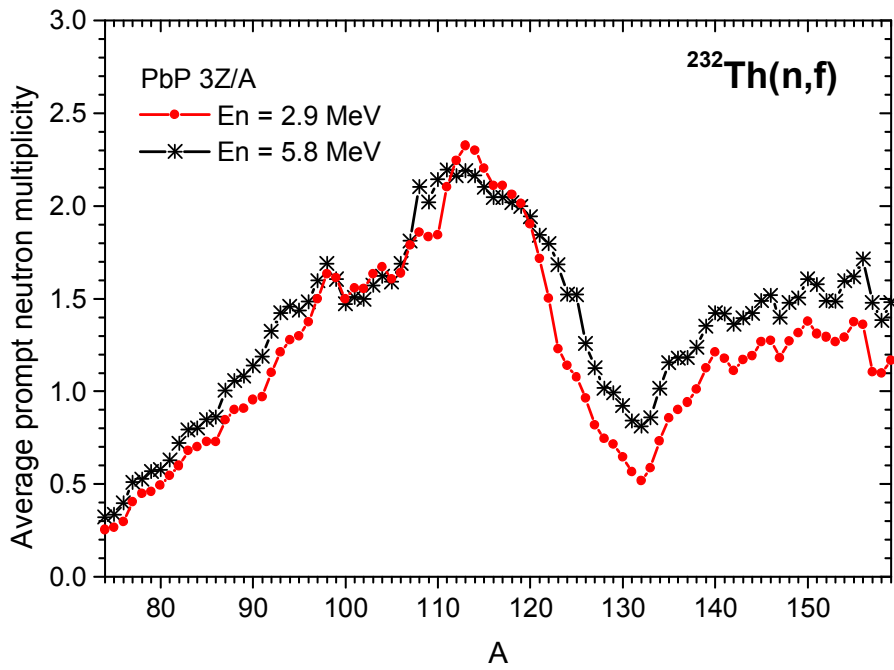


Fig.3: PbP results of $\bar{\nu}(A)$ at $E_n = 2$ MeV (red circles) and 5.8 MeV (black stars).

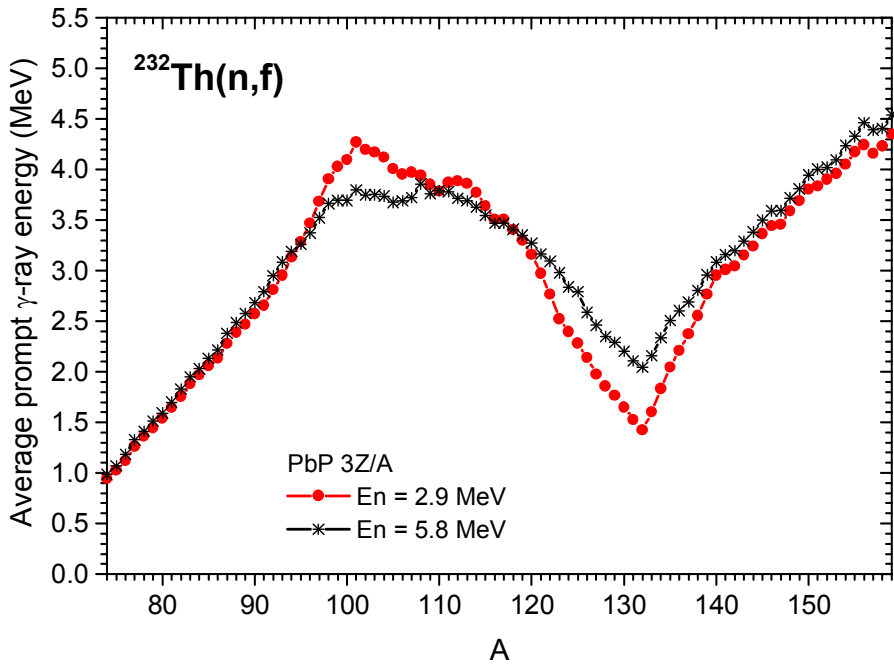


Fig.4: PbP results of average prompt gamma-ray energy as a function of fragment mass number at $E_n = 2.9$ MeV (red circles) and 5.8 MeV (black stars).

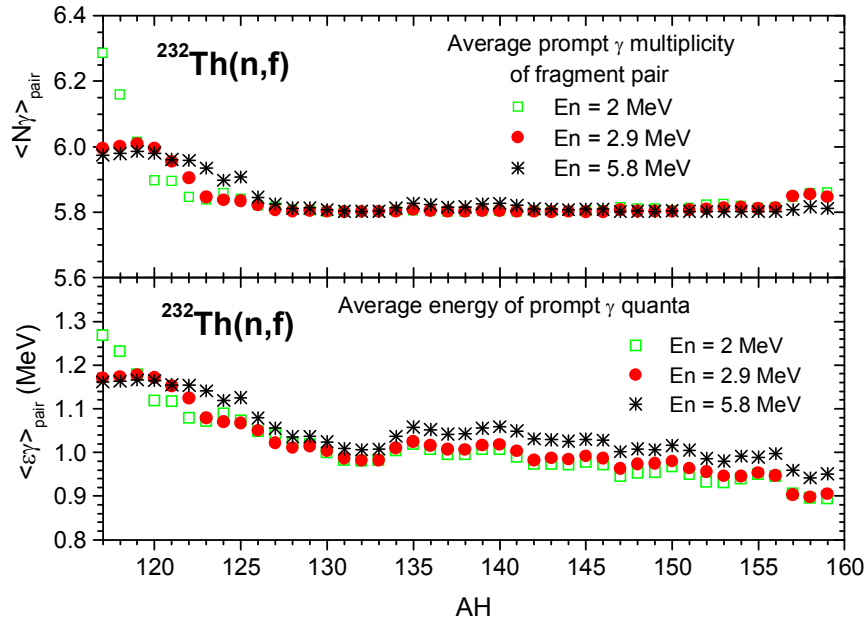


Fig.5: Upper part: average prompt gamma multiplicity of fragment pair as a function of A_H at $E_n = 2$ MeV (open green squares), 2.9 MeV (red circles) and 5.8 MeV (black stars). Lower part: single gamma quantum average energy $\langle \epsilon_\gamma \rangle_{\text{pair}}$ as a function of A_H (same symbols and colors as in the upper part)

The single gamma quantum average energy $\langle \epsilon_\gamma \rangle_{\text{pair}}$ (obtained as $\langle E_\gamma \rangle_{\text{pair}} / \langle N_\gamma \rangle_{\text{pair}}$) is plotted as a function of A_H in the lower part of Fig.5 with the same symbols as in the upper part. The $\langle \epsilon_\gamma \rangle_{\text{pair}}$ increase with E_n is visible and can be understood in the frame of a larger available phase space allowing a larger number of relatively high energy gamma-rays to be emitted [6].

3.2 PbP calculations of total average quantities as a function of incident neutron energy

The total average prompt neutron multiplicity $\langle \nu_p \rangle_{\text{tot}}$ and prompt gamma-ray energy $\langle E_\gamma \rangle_{\text{tot}}$ are obtained by averaging the PbP results as a function of fragment pair over charge distribution and the experimental distributions of Sergachev taken from EXFOR [20].

The $\langle \nu_p \rangle_{\text{tot}}$ results at the incident energies for which experimental $Y(A)$ exist in EXFOR [20] are plotted with full red circles in Fig.6. PbP calculations of $\langle \nu_p \rangle_{\text{tot}}$ were also done at other incident energies between 3 and 5.8 MeV by averaging over the experimental $Y(A)$ data measured at 3 MeV (in the cases of $E_n = 3.5$ MeV, 4 MeV and 4.5 MeV) and at 5.8 MeV (in the case of $E_n = 5$ MeV). These results are plotted with open red circles with a cross center. As it can be seen in Fig.6 the $\langle \nu_p \rangle_{\text{tot}}$ results are in good agreement with the experimental data from EXFOR [4] (plotted with different black and gray open symbols). The behaviour of experimental $\langle \nu_p \rangle_{\text{tot}}$ data exhibiting a visible increase at $E_n = 1.4 - 1.6$ MeV where the fission cross-section of ^{232}Th has very pronounced sub-barrier resonances is well reproduced by the PbP results at 1.6 and 1.75 MeV.

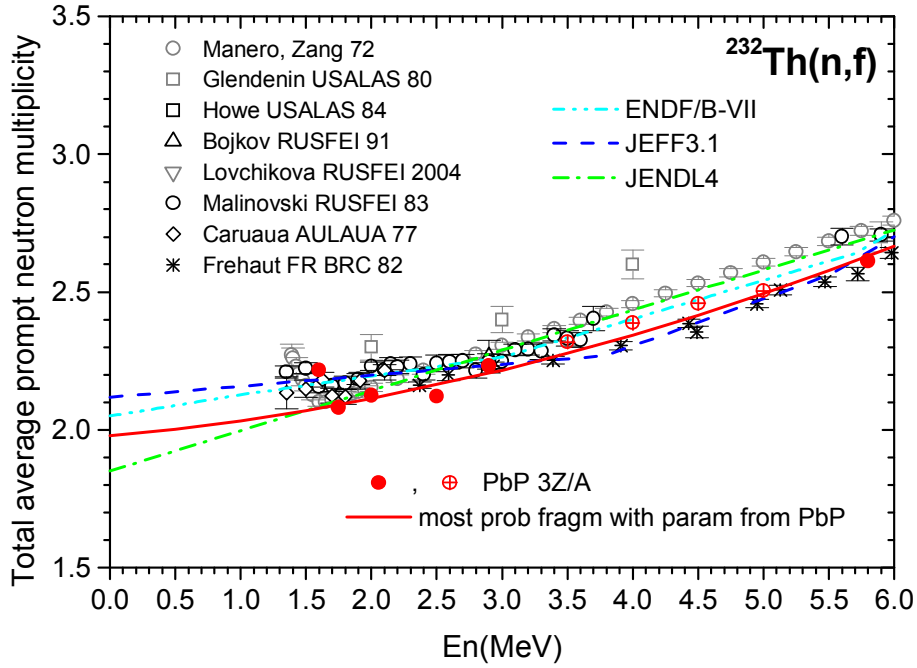


Fig.6: $\langle v_p \rangle_{\text{tot}}$ of $^{232}\text{Th}(n,f)$ in the E_n range of the first chance: experimental data from EXFOR (different open symbols), recent evaluations (different dashed and dotted lines), PbP calculation at the E_n values where experimental fragment distributions exist (full red circles) and at other E_n using the experimental distributions at 3 MeV and 5.8 MeV (red open circles with a cross center), most probable fragmentation result (red solid line).

The PbP result of total average prompt gamma-ray energy plotted in **Fig.7** (with the same symbols as in Fig.6) is in good agreement with the unique experimental data of Fréhaut [6] (full black squares) and also exhibits an increase around the energies where the fission cross-section has pronounced sub-barrier resonances.

Total average prompt gamma multiplicity $\langle N_\gamma \rangle$ and single prompt γ quantum average energy $\langle \varepsilon_\gamma \rangle$ (also obtained by averaging over the charge distribution and the experimental distributions from [20]) are plotted with red squares in the upper and lower parts of **Fig.8**, respectively. As can be seen, $\langle N_\gamma \rangle$ is practically constant and $\langle \varepsilon_\gamma \rangle$ is increasing with E_n , confirming the behaviours reported by Fréhaut [6] for three fissioning systems $^{235}\text{U}(n,f)$, $^{237}\text{Np}(n,f)$ and $^{232}\text{Th}(n,f)$.

The PbP results of PFNS, obtained by using $\sigma_c(\varepsilon)$ from optical model calculations with the Becchetti-Greenlees parameterization, describe very well the existing experimental data at $E_n = 2$ MeV and 2.9 MeV (taken from EXFOR [5]), as seen in **Figs. 9** and **10**, respectively. Calculations done by using the optical potential parameterization of Koning-Delaroche led to spectrum shapes in less good agreement with the experimental data.

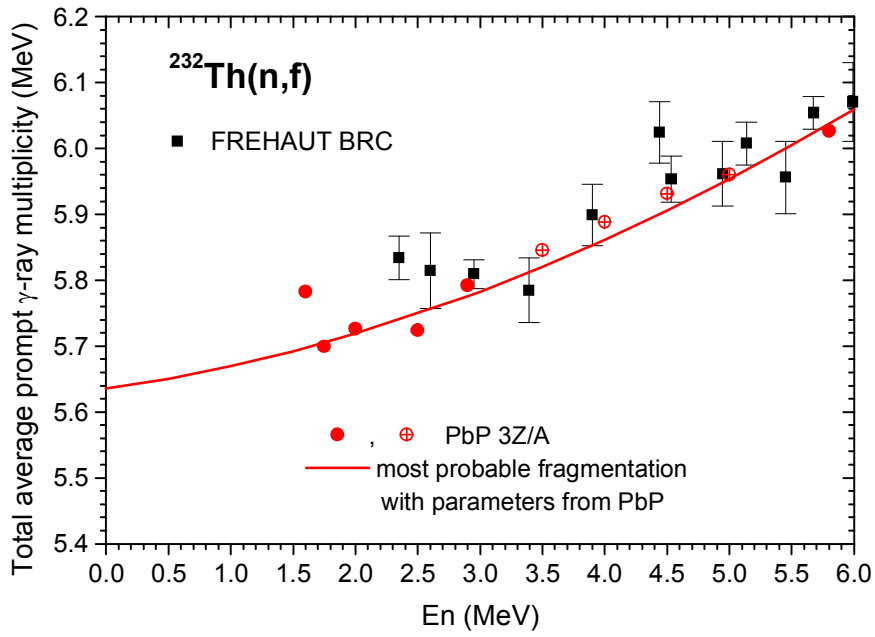


Fig.7: Total average prompt γ -ray energy as a function of E_n : experimental data of Fréhaut (full squares), PbP calculations (red circles) and most probable fragmentation result (red line).

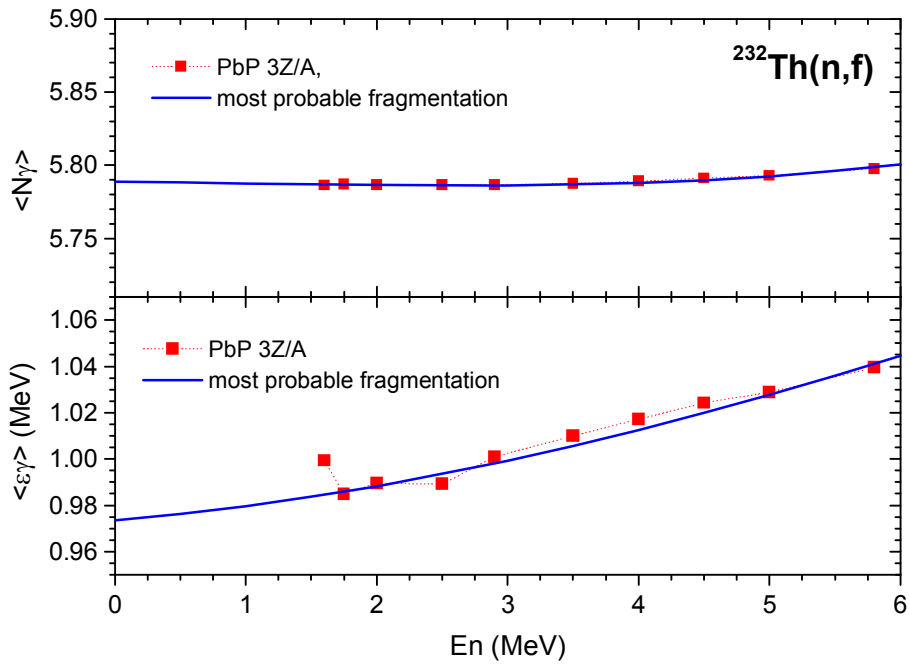


Fig.8: PbP result (red squares) and most probable fragmentation result (blue line) of total average prompt gamma multiplicity (upper part) and of single γ quantum total average energy (lower part) as a function of E_n

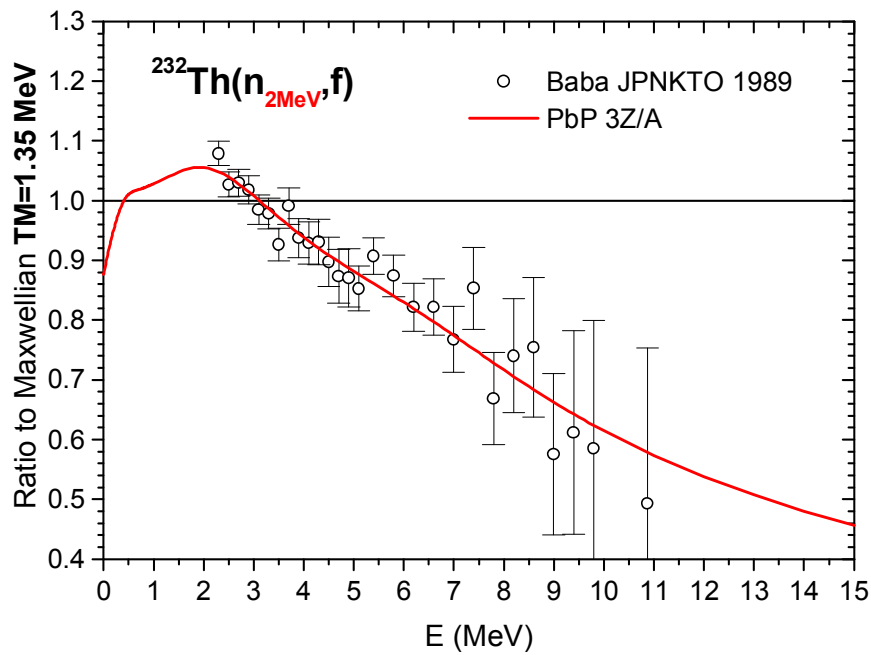


Fig.9: PbP result of PFNS at $E_n = 2$ MeV given as ratio to Maxwellian in comparison with the experimental data from EXFOR.

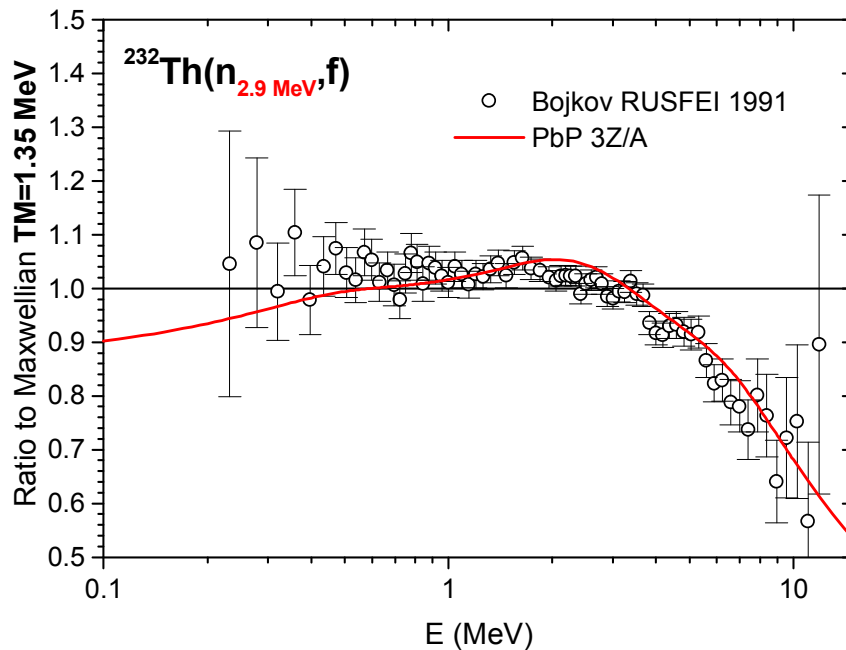


Fig.10: PbP result of PFNS at $E_n = 2.9$ MeV given as ratio to Maxwellian in comparison with the experimental data from EXFOR.

PbP calculations of total average quantities characterizing the fission fragments are plotted with full red circles in **Fig.11** as follows: the total average energy release $\langle E_r \rangle$ in the upper part, the average neutron separation energy from fragments $\langle S_n \rangle$ in the middle part and the average level density parameter of fragments $\langle a \rangle$ (given traditionally as $\langle C \rangle = A_0 / \langle a \rangle$ where A_0 is the mass number of the fissioning nucleus) in the lower part. Variations of these

quantities around the energies of sub-barrier fission cross section resonances are visible. Appropriate fits are also given in the figure.

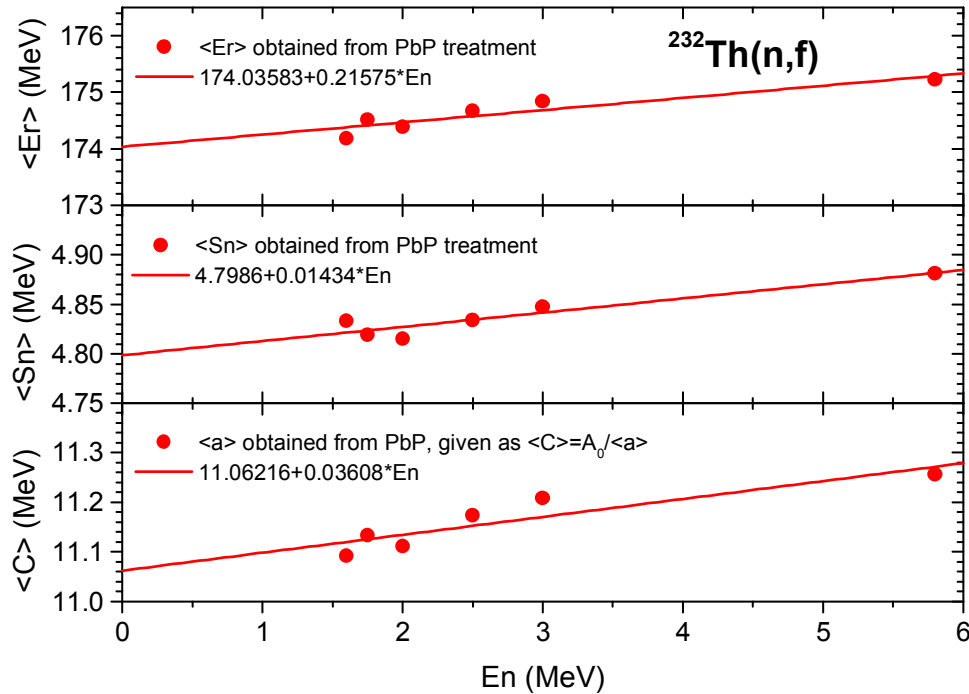


Fig.11: Total average values of $\langle Er \rangle$ (upper part), $\langle Sn \rangle$ (middle part) and $\langle C \rangle = A_0 \langle a \rangle$ (lower part) obtained from the PbP treatment as a function of E_n (red circles) and appropriate fits (red lines).

In **Fig.12** the experimental $\langle TKE \rangle$ data sets from EXFOR [35] are plotted with different symbols as indicated in the figure legend. An appropriate second order polynomial fit is also given. As can be seen, the experimental $\langle TKE \rangle$ data exhibit visible non-statistical fluctuations in the E_n range 1.3 MeV – 2.4 MeV where the fission cross-section has pronounced sub-barrier resonances.

The correlation between the sub-barrier fission cross-section resonances and the non-statistical fluctuations of fission fragment and prompt emission data around the resonance energies (already discussed for the fertile nuclei ^{238}U in [13] and ^{234}U in [12]) is observed in the case of $^{232}\text{Th}(n,f)$, too. Even if in the case of ^{232}Th the incident energies, for which fragment distributions were measured, do not cover a fine grid as in the cases of $^{238,234}\text{U}(n,f)$, the effect remains visible.

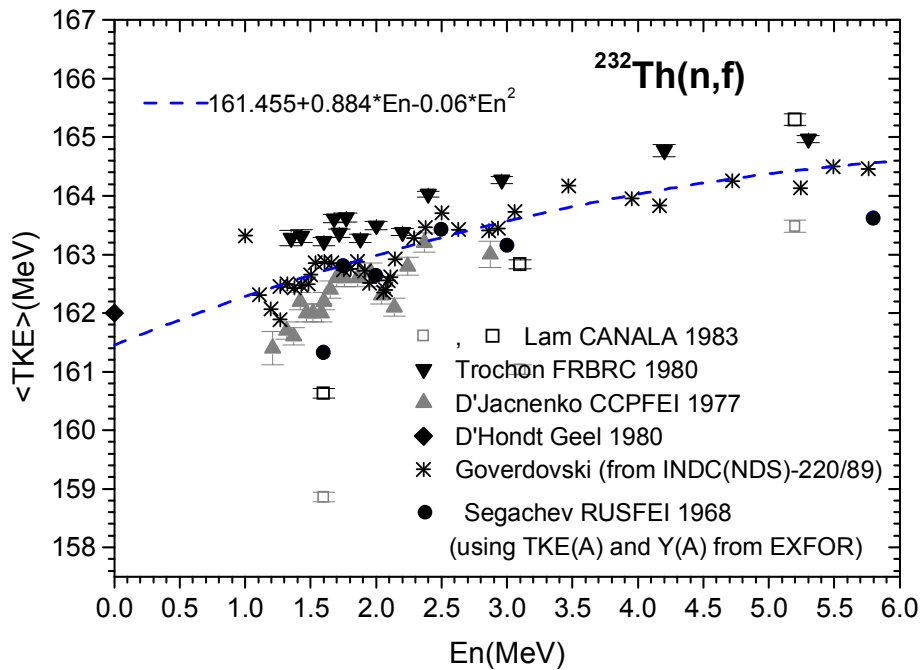


Fig.12: Experimental $\langle TKE \rangle$ data of $^{232}\text{Th}(n,f)$ taken from EXFOR (different symbols) and an appropriate fit (dashed line)

This correlated behaviour between the sub-barrier resonances of the fission cross-section (characterizing the pre-scission stage of fission) and the variation of total average quantities characterizing both the fission fragments and the prompt emission (post-scission stage) is emphasized in **Figs.13**.

In the upper part (Fig.13a) the fission cross-section of the latest released evaluations is plotted (ENDF/B-VII [36] with a red solid line, JEFF3.1 [24] with a green dash-dotted line and JENDL4 [23] with a blue dashed line). The three evaluations (obviously describing well the experimental data) exhibit very pronounced sub-barrier resonances between 1.3 – 2.4 MeV.

The variations of experimental $\langle TKE \rangle$ data in this E_n range are also visible (Fig.12 and Fig.13b).

The experimental prompt neutron multiplicity data (Fig.3c) exhibit a pronounced increase between 1.3-1.7 MeV (like a large resonance) that is supported by the PbP results at 1.6 MeV and 1.75 MeV.

Experimental data of total average prompt gamma-ray energy do not exist below 2.3 MeV, but the variation of the PbP result at 1.6 and 1.75 MeV shows the correlated behaviour, too.

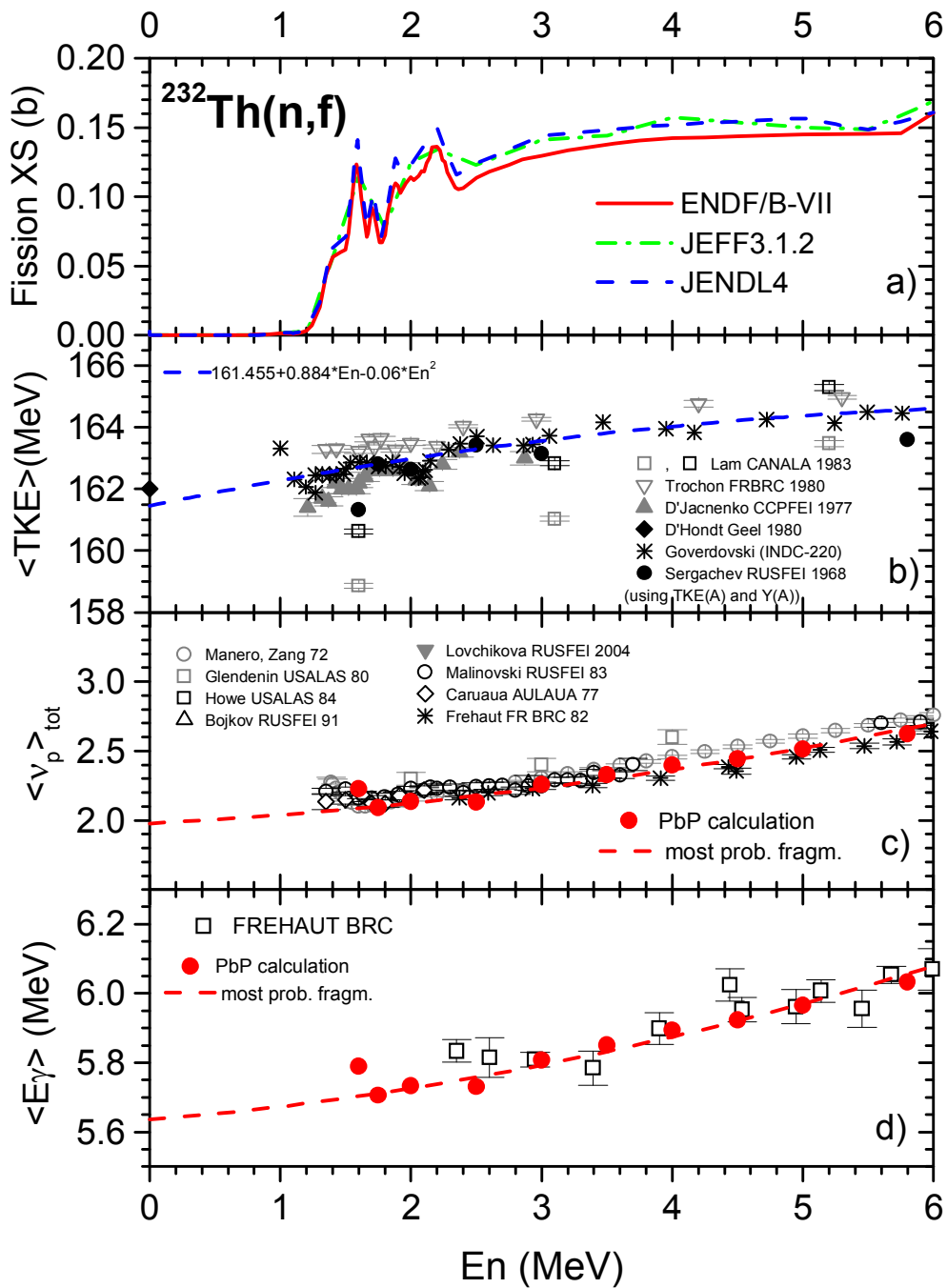


Fig.13: $^{232}\text{Th}(n,f)$ Illustration of the correlation between the sub-barrier resonant behaviour of the fission cross-section (the latest released evaluations in panel a) and the non-statistical fluctuations around the energies of resonances exhibited by total average quantities characterizing the fission fragments (e.g. $\langle\text{TKE}\rangle$ in panel b) and the prompt emission (the total average prompt neutron multiplicity in panel c and the prompt gamma-ray energy in panel d).

3.3 Calculations in the frame of the most probable fragmentation approach

The dependences on E_n of total average quantities $\langle E_r \rangle$, $\langle S_n \rangle$, $\langle a \rangle$ (obtained from the fit to

PbP results, see Fig.11) and of $\langle \text{TKE} \rangle$ (obtained by fitting to experimental data over the En range of the first fission chance, see Fig.12) allow the use of the most probable fragmentation approach. The obtained results of $\langle v_p \rangle_{\text{tot}}$ and $\langle E_\gamma \rangle_{\text{tot}}$, describing well the experimental data, are plotted with red solid lines in Figs.6 and 7, respectively. The most probable fragmentation results of total average $\langle n_\gamma \rangle$ and $\langle \varepsilon_\gamma \rangle$ are also given with blue lines in Fig.8 (upper and lower part, respectively).

The most probable fragmentation results of PFNS at En = 2 MeV and 2.9 MeV are compared with the experimental data in **Figs.14** and **15**, respectively. Spectrum calculations were done in two cases as following:

- using compound nucleus cross-sections of the inverse process $\sigma_c(\varepsilon)$ provided by optical model calculations with the parameterization of Becchetti-Greenlees [17], the resulted PFNS being given in the upper parts of Figs.14 and 15;
- using the formula $\sigma_c(\varepsilon) = \sigma_0(1 + \alpha/\sqrt{\varepsilon})$ proposed by Iwamoto [37], the PFNS results being given in the lower parts of Figs.14 and 15.

It is known that $\sigma_c(\varepsilon)$ has a major influence on the spectrum shape, this fact being visible in Figs.14, 15 too. Even if the spectrum shapes obtained by using $\sigma_c(\varepsilon)$ from optical model calculations and $\sigma_c(\varepsilon)$ of the Iwamoto formula are different, both PFNS results succeed to give an overall good description of experimental data at 2 MeV and 2.9 MeV. However, at En = 2 MeV the spectrum obtained by using $\sigma_c(\varepsilon)$ from optical model calculations seems to describe better the experimental data between 2 and 5 MeV (see Fig.14). At En = 2.9 MeV it seems that PFNS obtained by using $\sigma_c(\varepsilon)$ of Iwamoto describes better the experimental data around 2 MeV (see Fig.15).

To perform prompt emission calculations at higher incident energies where multiple fission chances are involved (for details see Refs. [27, 38] and references therein), total average values of model parameters ($\langle \text{Er} \rangle$, $\langle \text{TKE} \rangle$, $\langle \text{Sn} \rangle$, $\langle a \rangle$) of secondary compound nuclei undergoing fission as well as the fission probabilities (expressed as fission cross-section ratios) are needed.

In the present case prompt emission calculations being done up to the incident neutron energy of 20 MeV, only four fissioning nuclei $^{233-230}\text{Th}$ of the main nucleus chain are involved. For the main fissioning nucleus ^{233}Th the average model parameters (depending on En) resulted from the PbP treatment are used. The average model parameters of secondary nuclei $^{232,231,230}\text{Th}$ are taken from the systematic of Los Alamos input parameters of Ref. [22]. Unfortunately experimental prompt emission data of neutron-induced reactions in which the nuclei $^{232, 231, 230}\text{Th}$ are the main compounds, necessary to verify these parameters, are almost missing. The unique exception is $^{230}\text{Th}(n,f)$ for which experimental prompt neutron multiplicity data exist in EXFOR [39]. These data allow the verification of the average model parameters of ^{231}Th (acting as the third chance in the studied reaction $n+^{232}\text{Th}$) by performing prompt emission calculations for the reaction $^{230}\text{Th}(n,f)$. The obtained prompt neutron multiplicity result describes very well these experimental data as it can be seen in **Fig.16**.

Prompt emission calculations for ^{232}Th up to En = 20 MeV were done using the fission cross-section ratios (RF) from the evaluations JENDL4 [23] and JEFF3.1 [24] plotted in **Fig.17**. The use of fission cross-section ratios from JEFF3.1.2 leads to a prompt neutron multiplicity result that underestimates the experimental data above 10 MeV, see **Fig.18**. The RF of JENDL4 lead to prompt emission results in very good agreement with all existing experimental data, as follows.

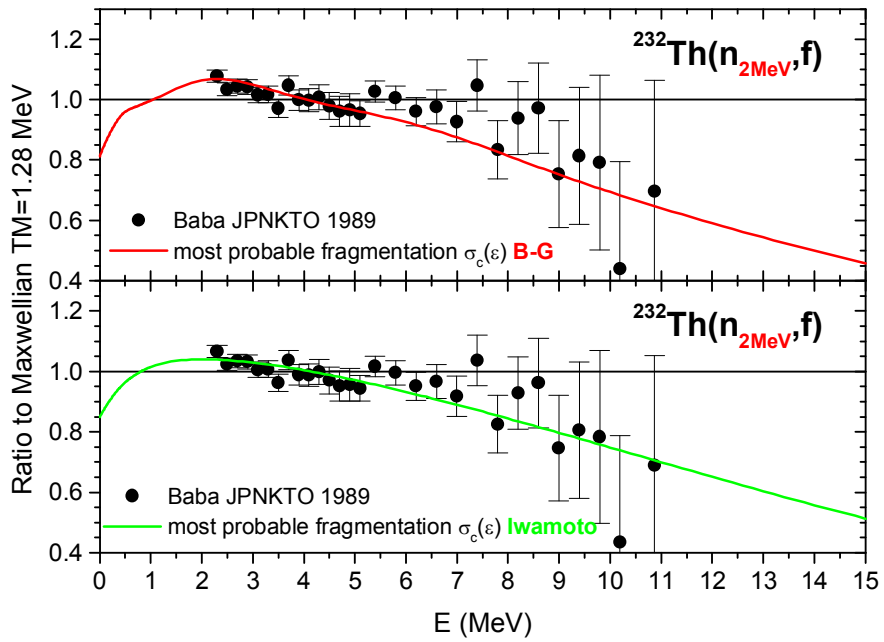


Fig.14: Most probable fragmentation result of PFNS at $E_n = 2$ MeV (upper part with $\sigma_c(\epsilon)$ from optical model calculation with the Becchetti-Greenlees parameterization, lower part with $\sigma_c(\epsilon)$ given by the formula of Iwamoto) in comparison with experimental data from EXFOR. Spectra are given as ratio to a Maxwellian spectrum.

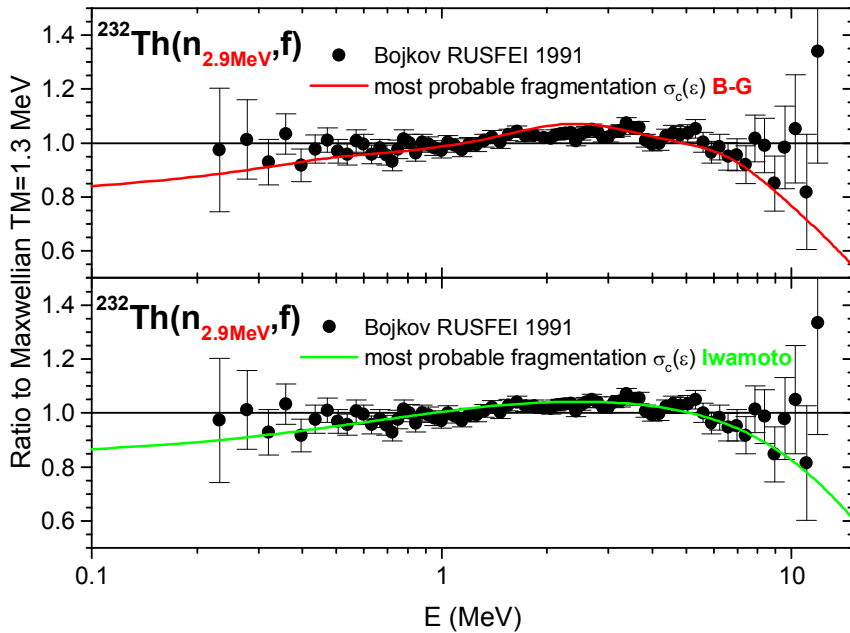


Fig.15: Most probable fragmentation result of PFNS at $E_n = 2.9$ MeV (upper part with $\sigma_c(\epsilon)$ from optical model calculation with the Becchetti-Greenlees parameterization, lower part with $\sigma_c(\epsilon)$ given by the formula of Iwamoto) in comparison with experimental data from EXFOR. Spectra are given as ratio to a Maxwellian spectrum.

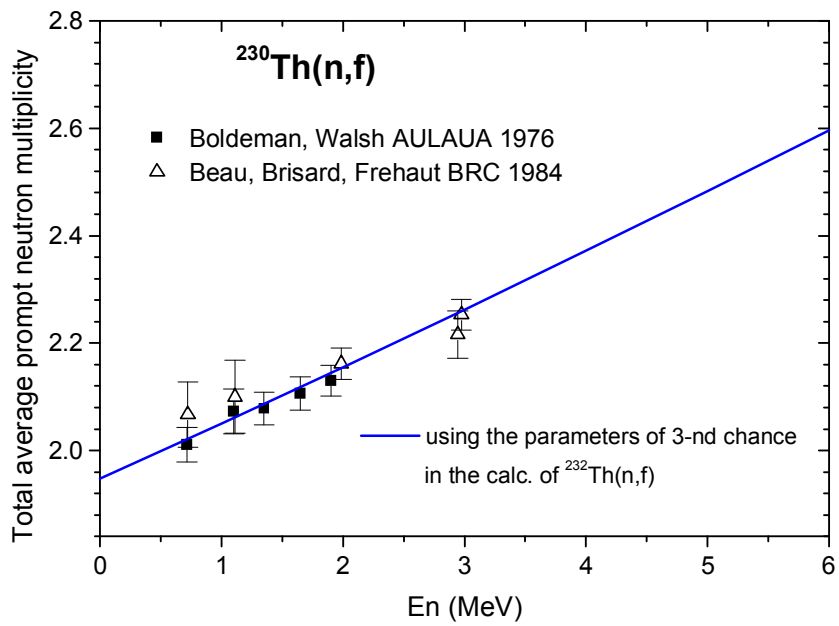


Fig.16: Most probable fragmentation results of total average prompt neutron multiplicity of ²³⁰Th(n,f) in comparison with experimental data form EXFOR: This result is obtained by using the average values of parameters of ²³¹Th acting as the third fission chance in the reaction n+²³²Th

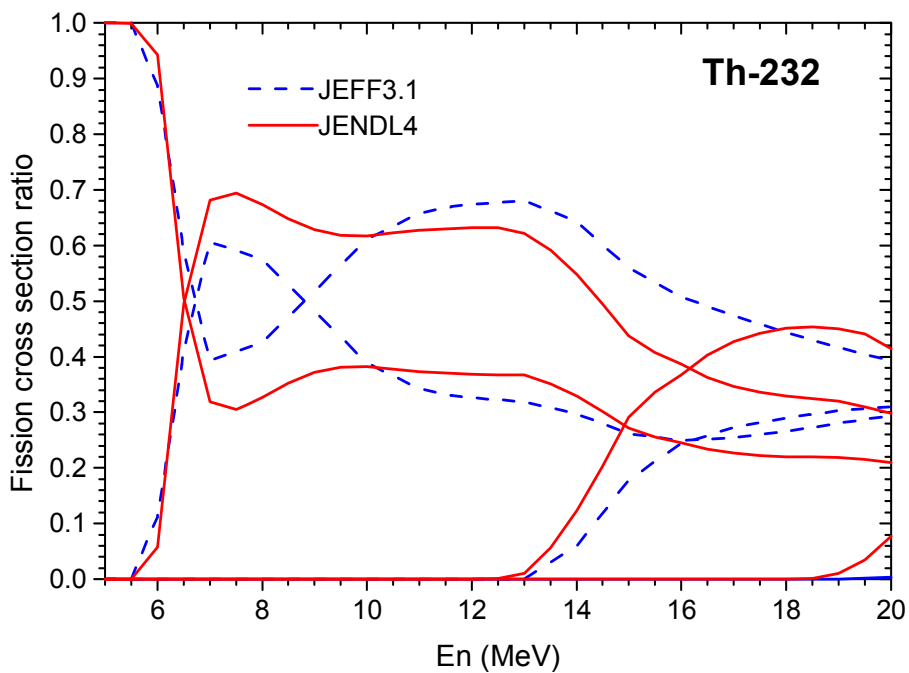


Fig.17: Fission cross-section ratios (RF) of ²³²Th from the evaluations JENDL4 (red solid lines) and JEFF3.1 (blue dashed lines)

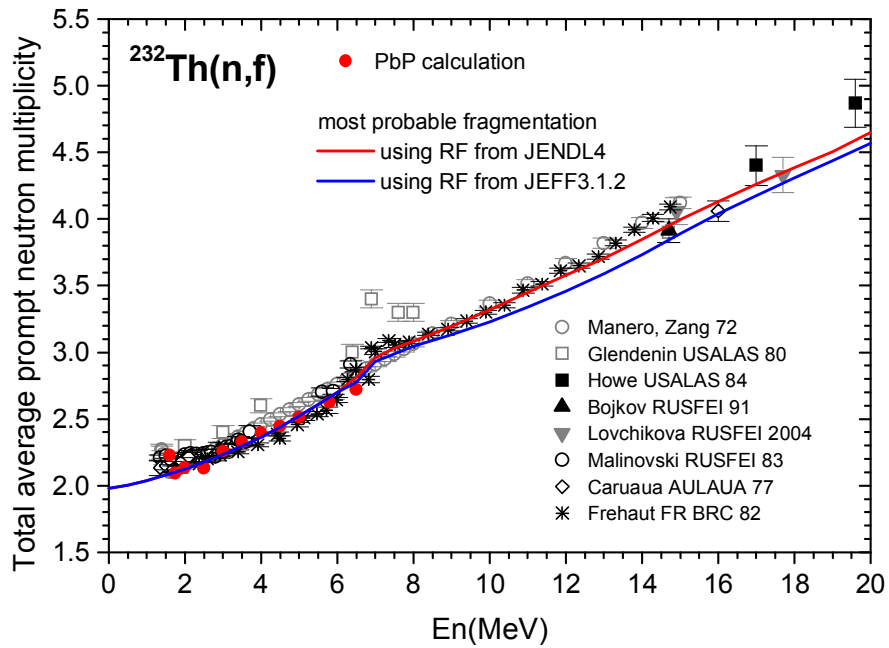


Fig.18: Total average prompt neutron multiplicity calculations using RF from JENDL4 (red line) and from JEFF3.1 (blue line) in comparison with experimental data. The PbP result is also given (red circles).

In **Fig.19** the $\langle v_p \rangle_{\text{tot}}$ calculation up to 20 MeV is plotted with a red solid line in comparison with the experimental data from EXFOR [4] (different black and gray symbols) and the latest released evaluations ENDF/B-VII [10] (cyan dashed line), JEFF3.1.2 [8] (blue dash dotted line) and JENDL4 [7] (green dotted line). As it can be seen the present $\langle v_p \rangle_{\text{tot}}$ result describes very well the experimental data over the entire energy range up to 20 MeV, including the sudden (abrupt) multiplicity increase at 7 MeV (where the second fission chance is opening).

The $\langle E_\gamma \rangle_{\text{tot}}$ result plotted with a red solid line in **Fig.20** gives a very good description of experimental data of Fréhaut [6].

More detailed results of prompt neutrons and gamma-ray emission (including the contribution of fission chances) are given in **Figs.21 and 22**.

In the case of ^{232}Th experimental prompt neutron spectrum data at high incident energies exist in EXFOR [5] (measured by Lovchikova et al. at 14.6 MeV and 17.7 MeV and by Bojkov et al at 14.7 MeV).

Looking at the behaviour of experimental data at $E_n = 14.6$ and 14.7 MeV plotted in **Figs.23a, b** (data of Lovchikova with full gray circles and of Bojkov with open squares) a lump is observed around 8 MeV. Similar lumps (change in slope) were observed in the experimental spectrum data at high incident neutron energies of other fissioning nuclei, too (e.g. $^{235}\text{U}(n,f)$ at 14.7 MeV [40]). This behaviour of experimental spectrum data can be explained by the contribution of neutrons evaporated prior to the scission, meaning the neutron spectra of (n,xn) reactions (for details see Ref. [40] and references therein). This kind of lump is also reproduced with the CCONE code in the JENDL4 evaluation [7].

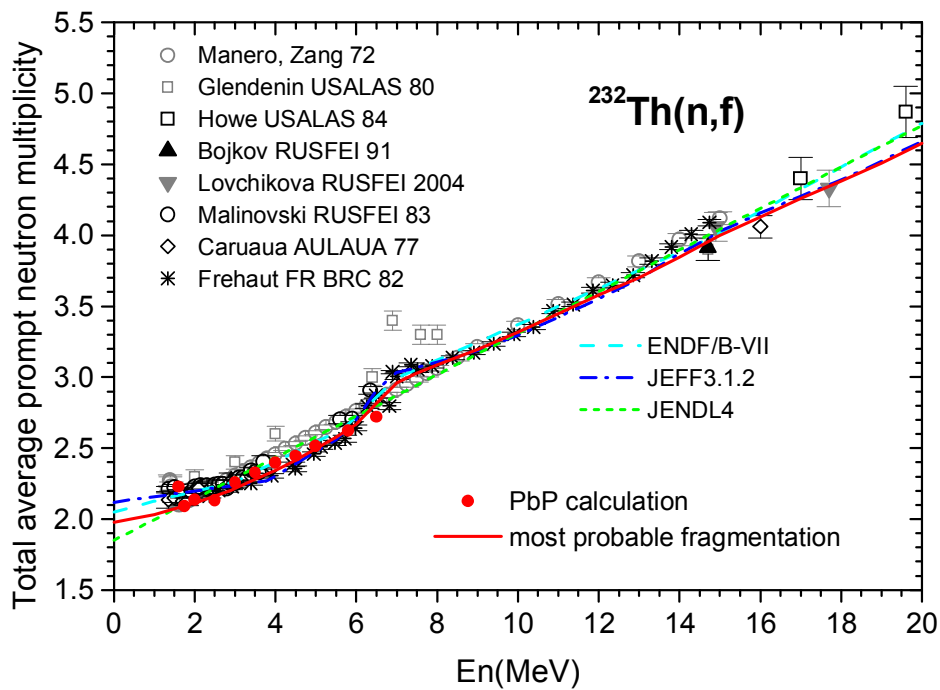


Fig.19: Total average prompt neutron multiplicity of $^{232}\text{Th}(n,f)$ calculated by using RF of JENDL4 (red solid line) in comparison with experimental data (different black and gray symbols) and recent evaluations (different dashed and dotted lines). PbP results are also given with full red circles.

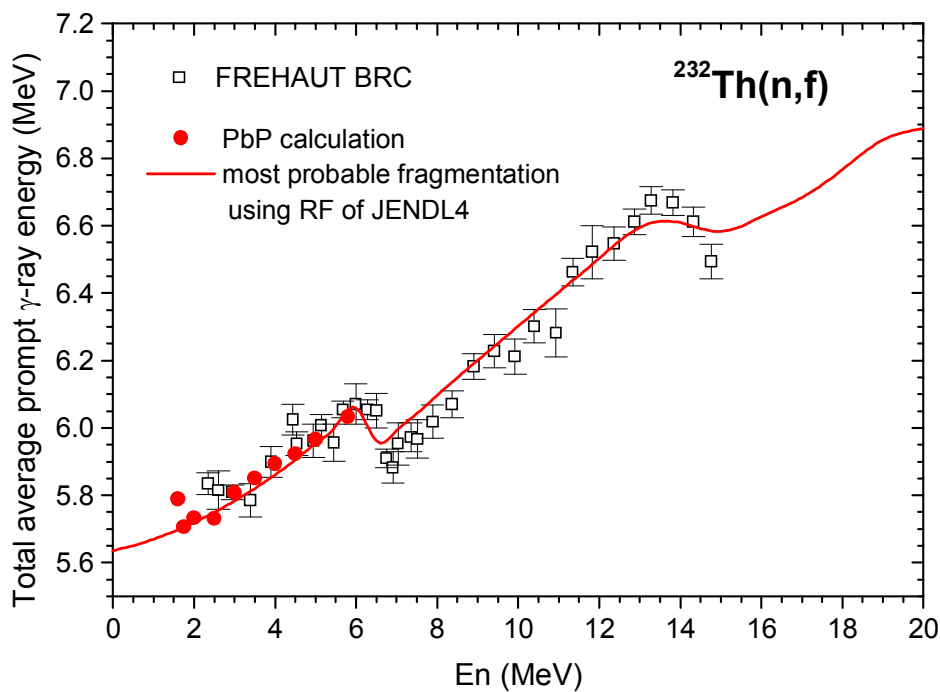


Fig.20: $\langle E_\gamma \rangle_{\text{tot}}$ calculation using RF of JENDL4 (red solid line) in comparison with experimental data of Fréhaut (open black squares). PbP results are also given with full red circles.

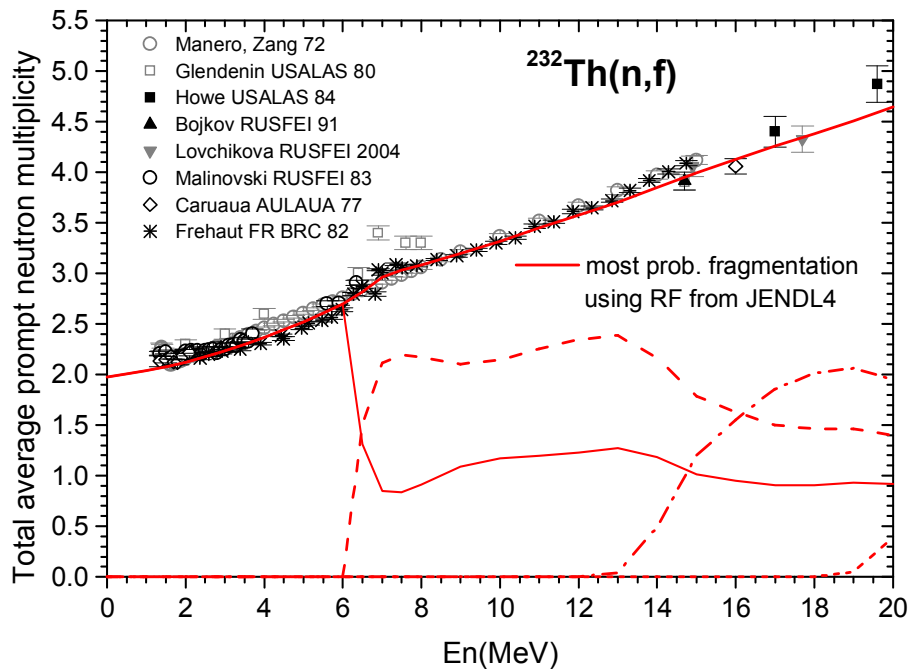


Fig.21 Average prompt neutron multiplicities of fission chances and the total average prompt neutron multiplicity in comparison with experimental data. The result is obtained by using RF from JENDL4.

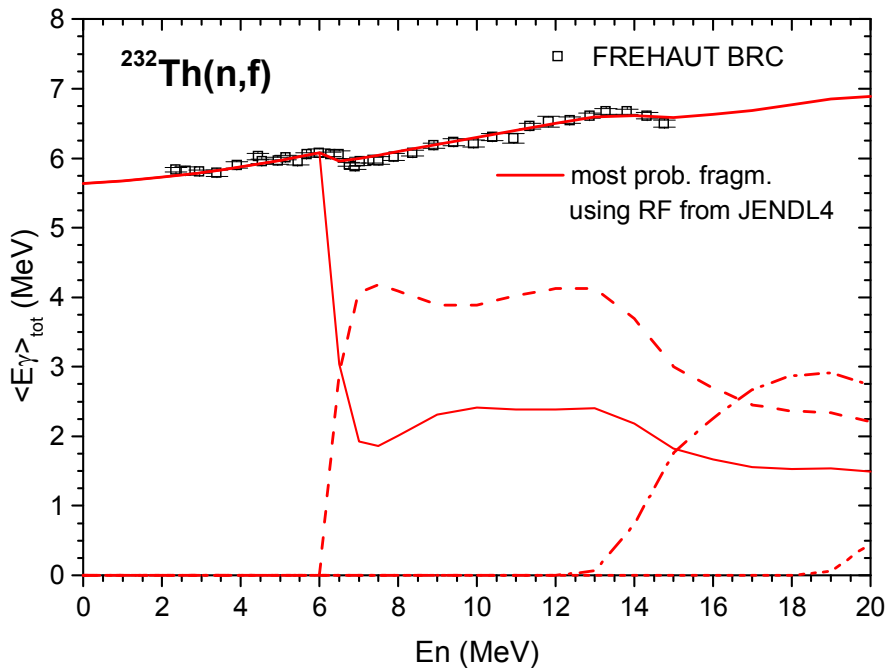


Fig.22: $\langle E_\gamma \rangle$ of fission chances and the total average $\langle E_\gamma \rangle_{\text{tot}}$ in comparison with experimental data of Fréhaut. The result is obtained by using RF from JENDL4.

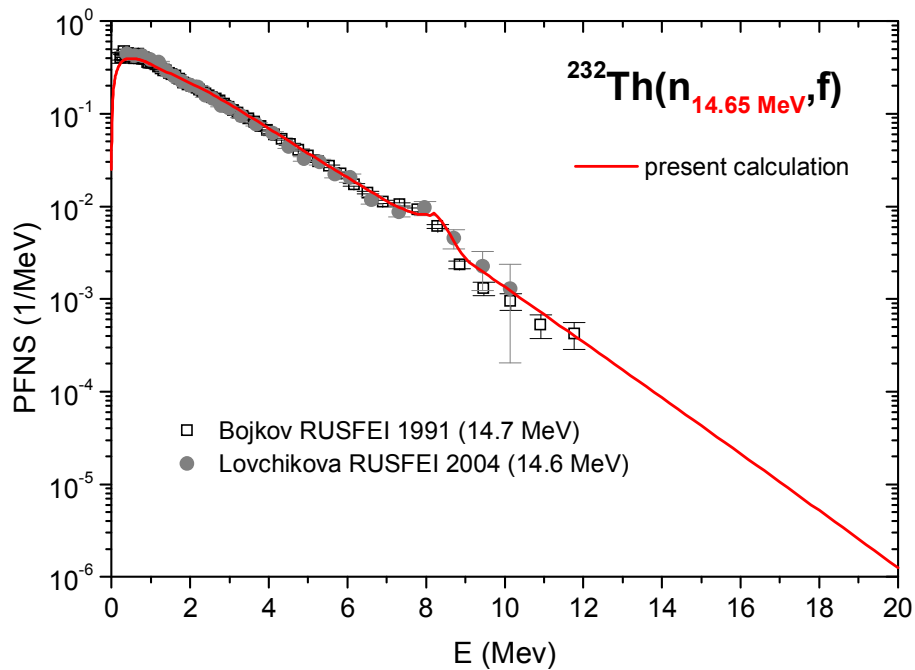


Fig.23a: PFNS calculation at $E_n = 14.65$ MeV in comparison with experimental data of Bojkov et al (open squares) and of Lovchikova et al (full circles).

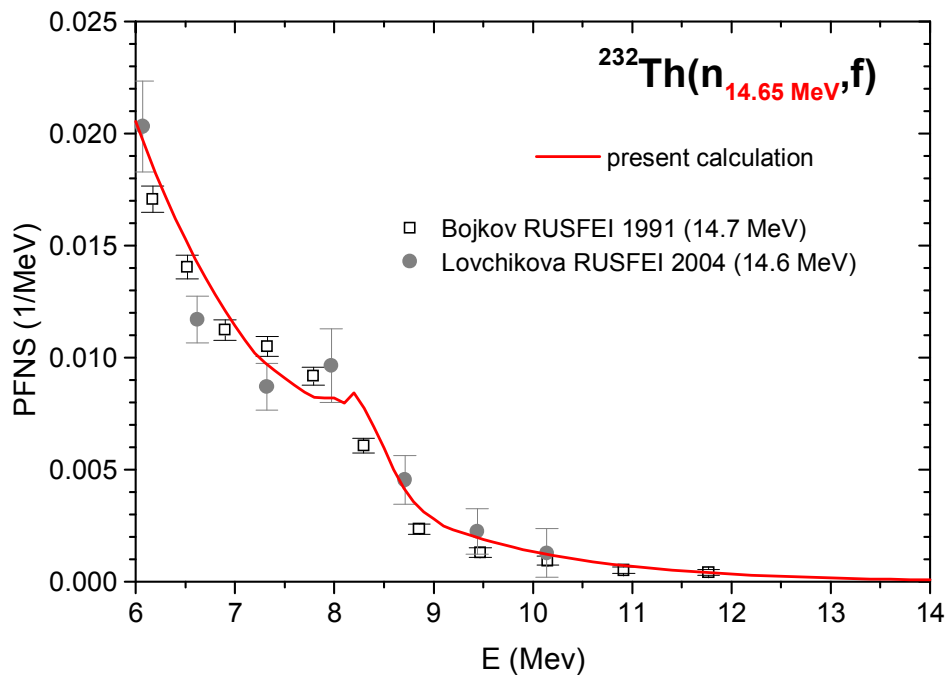


Fig.23b: PFNS calculation at $E_n = 14.65$ MeV in comparison with experimental data of Bojkov et al (open squares) and of Lovchikova et al (full circles). The high E region of the spectrum is focused (linear scales).

In the present case the neutron induced reaction calculations reported by [Sin et al \[25\]](#) (using a refined statistical model for fission with sub-barrier effects included in the code EMPIRE and a triple-humped barrier for the discrete part of the transition state spectrum) were

reproduced by using the same model (included in the improved version of the code GNASH, for details see Refs. [26, 27]) and the same parameters as in Ref. [25].

The (n,xn) spectra provided by GNASH, from which the contribution of neutrons leading to excitation energies of the residual nucleus less than the fission barrier height were subtracted, are used to describe the neutrons evaporated prior to the scission.

The calculated PFNS at $E_n = 14.65$ MeV succeeds to describe well the behaviour of experimental data around 8 MeV as it can be seen in **Fig.23a** (where the entire spectrum is plotted in logarithmic scale) and especially in **Fig.23b** where only the high energy part of the spectrum is zoomed in linear scale.

The PFNS result at $E_n = 17.7$ MeV also describes well the experimental data as it can be seen in **Fig.24a**. The high energy part of this spectrum is zoomed in **Fig.24b** (linear scale). The lump at around 11.5 MeV exhibited by the present calculation cannot be confirmed by the experimental data because they are too scarce (experimental points around 11.5 MeV existing only at 10.8 MeV and 11.9 MeV).

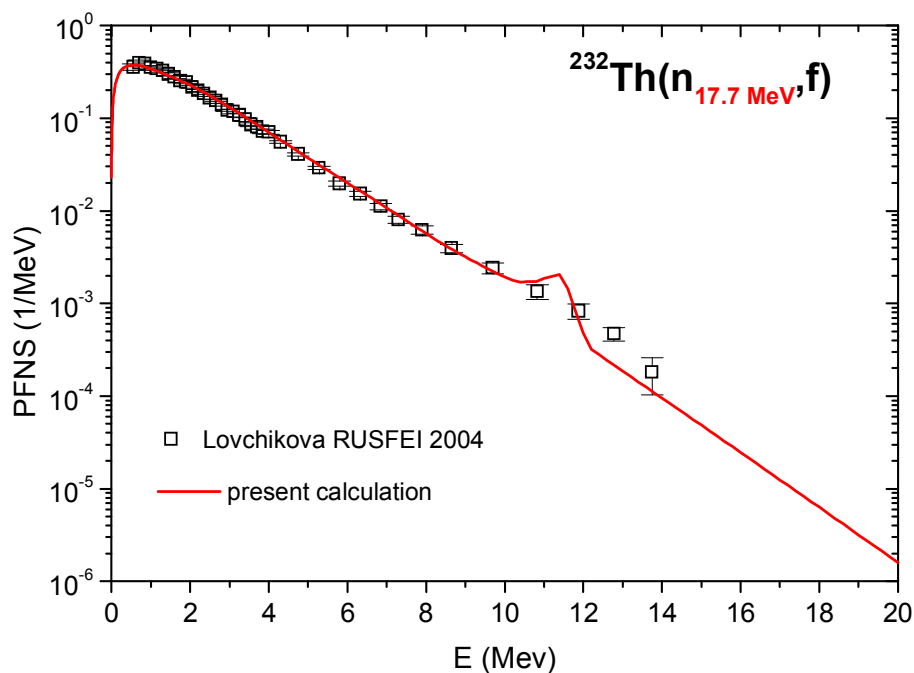


Fig.24a: PFNS calculation at $E_n = 17.7$ MeV in comparison with experimental data from EXFOR

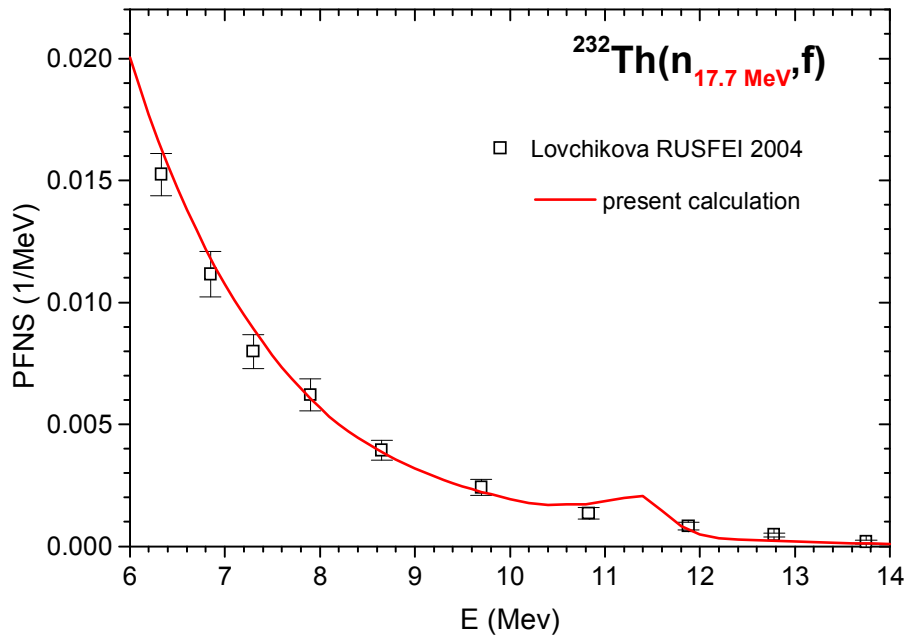


Fig.24b: PFNS calculation at $E_n = 17.7$ MeV in comparison with experimental data from EXFOR. The high E region of the spectrum is focused (linear scales).

In **Fig.25** the first order moments $\langle E \rangle$ (average energies of prompt neutrons) of present spectrum calculations (red circles connected with a solid line) and of spectra from the latest evaluations JENDL4 (blue diamonds connected with a dashed line) and JEFF3.1.2 (green triangles connected with a dash dotted line) are plotted in comparison with a few experimental data found in EXFOR [41] (different black symbols).

The first order moments of present PFNS and of both evaluations are in overall agreement with these data (excepting the data at 7 MeV and the two experimental points at 14.6 MeV and 14.7 MeV that are underestimated and overestimated respectively by all $\langle E \rangle$ results). In the E_n range where only the first chance is involved the present $\langle E \rangle$ results are a little bit higher than the evaluations but remaining in the error bar limits. The present $\langle E \rangle$ result and the JEFF3.1.2 evaluation are in agreement with the experimental data at 17.7 MeV, while the JENDL4 evaluation is much higher.

The verification of spectrum normalization at the unity is illustrated in **Fig.26**: our calculation with full red circles, the JEFF3.1.2 evaluation with full green triangles and the JENDL4 evaluation with full blue diamonds. As it can be seen the present PFNS (that are results of a consistent model calculation without any adjustment) accomplish the normalization condition while PFNS of both evaluations visibly exceed the unity.

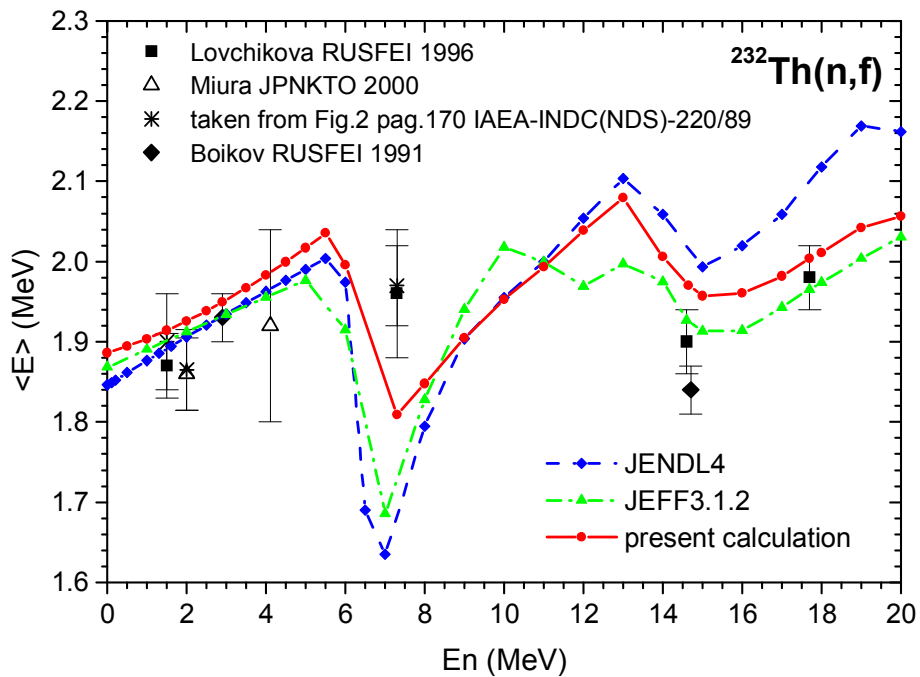


Fig.25: Average prompt neutron energy (first order momentum) $\langle E \rangle$ as a function of E_n : experimental data (different symbols), recent evaluations JENDL4 (blue diamonds connected with a dashed line) and JEFF3.1.2 (green triangles connected with a dash dotted line) and the present calculation (red circles connected with a solid line)

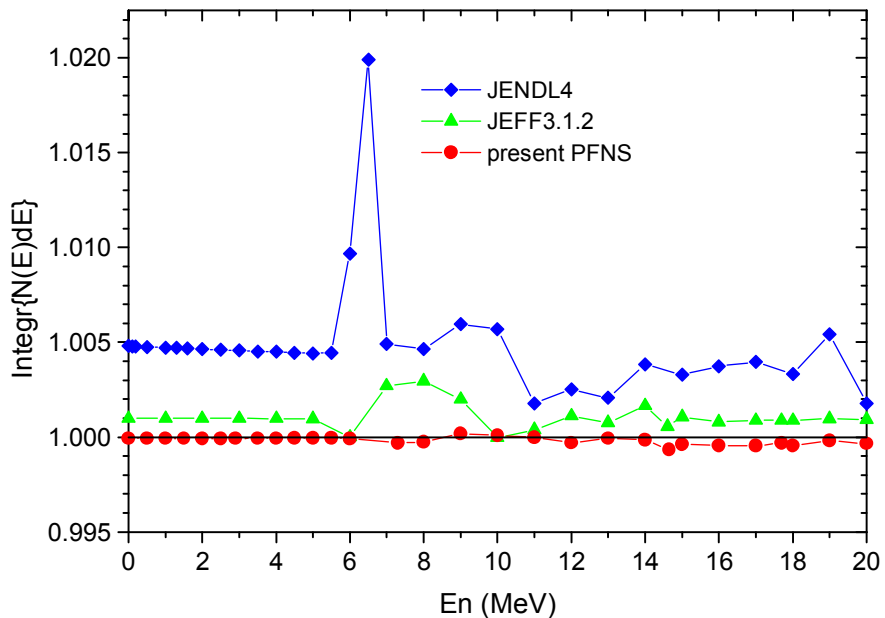


Fig.26: Verification of PFNS normalization to 1: JENDL4 (blue diamonds), JEFF3.1.2 (green triangles), present evaluation (red circles) and PbP calculation (red stars). The lines connecting the points are only to guide the eye.

4. Conclusions

Prompt neutron and gamma-ray emission data are obtained by a consistent model calculation. For the first time the experimental total average prompt gamma-ray energy data of $^{232}\text{Th}(n,f)$ are very well described by model calculations.

The total average prompt neutron multiplicity gives an excellent description of experimental data over the entire fast neutron energy range, including the variations around the energies of fission cross-section resonances and the sudden increase at the incident energy where the second fission chance is opening.

The $\bar{\nu}(A)$ behaviour consisting in the multiplicity increase with the incident energy for heavy fragments only, experimentally observed for $^{235}\text{U}(n,f)$ and $^{237}\text{Np}(n,f)$ and confirmed by model calculations, is supported by the PbP results of $\bar{\nu}(A)$ in the case of $^{232}\text{Th}(n,f)$, too.

The correlation between the sub-barrier resonances in the fission cross-section and the non-statistical variations of fragment and prompt emission data around the resonance energies, already discussed for the fertile actinides ^{238}U and ^{234}U , is confirmed by the present PbP results of $^{232}\text{Th}(n,f)$.

In the incident energy range where only the first fission chance is involved the PbP results of prompt neutron spectrum are in very good agreement with the existing experimental data.

At higher incident energies where multiple fission chances are involved, the lump around 8 MeV, exhibited by the experimental prompt neutron spectrum data measured at 14.6 MeV, is well described by the most probable fragmentation approach including the contribution of neutrons emitted prior to the scission given by the (n,xn) spectra provided by nuclear reaction calculations.

The results included in this report are published in

A.Tudora, “Prompt neutron and gamma-ray emission calculations for $^{232}\text{Th}(n,f)$ ”. *Nuclear Physics A* 916 (2013)79-101. <http://dx.doi.org/10.1016/j.nuclphysa.2013.07.011>

REFERENCES

- [1] A.Trkov, “Evaluated nuclear data for Th-U fuel cycle”, IAEA INDC(NDS)-447 (2003)
- [2] P.Schillebeeckx, A.Trkov, “Evaluated nuclear data for Th-U fuel cycle”, IAEA INDC(NDS)-0494 (2006).
- [3] R. Capote, “Prompt fission neutron spectra of actinides”, IAEA INDC(NDS)-0571 (2010)
- [4] EXFOR Nuclear Data Base (2013). Target Th-232, reactions (n,f), quantity MFQ, Prompt Nu. Available on-line <http://www-nds.iaea.org>
- [5] EXFOR Nuclear Data Base (2013). Target Th-232, reactions (n,f), quantity DE, entries 22112004 (Baba, 1989), 41110.008 (Bojkov, 1991), 41446004 (Lovchikova, 2004)
- [6] J.Fréhaut, IAEA INDC(NDS)-220 (1989) 99-111
- [7] JENDL4 Evaluated nuclear data file (2010). File ZA090232, MF=1, MT=456, MF=5, MT=18. Available on-line <http://www-nds.iaea.org>
- [8] JEFF3.1.2 Evaluated nuclear data file (2009). File ZA090232, MF=1, MT=456, MF=5, MT=18. Available on-line <http://www-nds.iaea.org>
- [9] VM.Maslov, Yu.V.Porodzinski, N.A.Tetereva, A.B.Kagalenco, N.V.Kornilov, M.Baba, A.Hasegawa, “Neutron data evaluation of ^{232}Th ” IAEA INDC(BLR)-16 (2003).

- [10] ENDF/B-VII Evaluated nuclear data file (2006) File ZA090232, MF=1, MT=456. Available on-line <http://www-nds.iaea.org>
- [11] A.Tudora, *Ann.Nucl.Energy* 53 (2013) 507-518
- [12] A.Tudora, F.-J.Hambsch, S.Oberstedt, “ $^{234}\text{U}(n,f)$ model description of sub-barrier fission cross-section resonances and calculation of prompt neutron emission data”, *Physics Procedia* (2013) ref PHPRO3615, DOI 10.1016/j.phpro.2013.06.011. “Model description of sub-barrier fission cross-section resonances and prompt neutron emission calculations for $^{234}\text{U}(n,f)$ ”, submitted to *Nucl.Phys.A*.
- [13] A.Tudora, F.-J.Hambsch, S.Oberstedt, *Nucl.Phys.A* 890-891 (2012) 77-101
- [14] RIPL3, Reference Input Parameter Library (2009). Segment 1 “Nuclear Masses and Deformations” database of Audi and Wapstra. Available on-line <<http://www-nds.iaea.org>>
- [15] RIPL3, Reference Input Parameter Library (2009). Segment 1 “Nuclear Masses and Deformations” database of Möller and Nix, Myers and Swiatecki. Available on-line <<http://www-nds.iaea.org>>
- [16] O. Bersillon, SCAT2 optical model computer code, OECD-NEA-DB-CPS package ID *NEA0859/07* (2011)
- [17] RIPL3, Reference Input Parameter Library (2009), electronic file from segment “Optical Model Parameters”, (Becchetti-Greenlees, Koning-Delaroche). Available on-line <<http://www-nds.iaea.org>>
- [18] C.Morariu, A.Tudora, F.-J.Hambsch, S.Oberstedt, C.Manailescu, *J.Phys G: Nucl.Part Phys.* 39 (2012) 055103
- [19] C.Wagemans, “*The Nuclear Fission Process*”, (1991) CRC Press Boca Raton (Chapter 8) p. 392-423
- [20] EXFOR Nuclear Data Base (2013). Target Th-232, reaction (n,f), quantity FY, Y(A), TKE(A) Sergachev et al, 1968 entries 40173002-40173007 (Y(A) and 40173008-40173013 (TKE(A)). Available on-line <http://www-nds.iaea.org>
- [21] D.G.Madland, J.R.Nix, *Nucl.Sci.Eng.* 81, (1982) 213-271
- [22] A.Tudora, *Ann.Nucl.Energy* 36 (2009) 72-84
- [23] JENDL4 Evaluated nuclear data file (2010). File ZA090232, MF=3, MT=18, 19, 20, 21, 38. Available on-line <http://www-nds.iaea.org>
- [24] JEFF3.1.2 Evaluated nuclear data file (2009). File ZA090232, MF=3, MT=18, 19, 20, 21, 38. Available on-line <http://www-nds.iaea.org>
- [25] M.Sin, R.Capote, A.Ventura, M.Herman, P.Oblozinsky, *Phys.Rev.C* 74 (2006) 014608
- [26] G.Vladuca, F.-J.Hambsch, A.Tudora, S.Oberstedt, A.Oberstedt, F.Tovesson, D.Filipescu, *Nucl.Phys.A* 740 (2004) 3-19
- [27] G.Vladuca, A.Tudora, B.Morillon, D.Filipescu, *Nucl.Phys.A* 767 (2006) 112-137
- [28] A.Tudora, *Ann.Nucl.Energy* 33 (2006) 1030-1038
- [29] A.Tudora, *Ann.Nucl.Energy* 35 (1) (2008) 1-10
- [30] EXFOR Nuclear Data Base (2012). Target U-235, reaction (n,f), quantity MFQ: entries 21834009 and 21834010 (Naqvi and Mueller). Available on-line <http://www-nds.iaea.org>
- [31] EXFOR Nuclear Data Base (2012). Target Np-239, reaction (n,f), quantity MFQ: entries 21834016, 21834017, 21661002, 21661003 (Mueller and Naqvi). Available on-line <<http://www-nds.iaea.org>>
- [32] O.Litaize, O.Serot, *Phys.Rev.C* 82 (2010) 054616
- [33] C.Manailescu, A.Tudora, F.-J.Hambsch, C.Morariu, S.Oberstedt, *Nucl.Phys.A* 867 (2011) 12-40
- [34] K.-H.Schmidt, B.Jurado, *Phys.Rev.Lett.* 104 (2010) 212501
- [35] EXFOR Nuclear Data Base (2013). Target Th-232, reaction (n,f), quantity E, AKE-FF. Available on-line <http://www-nds.iaea.org>
- [36] ENDF/B-VII Evaluated nuclear data file (2006). File ZA090232, MF=3, MT=18.

Available on-line <http://www-nds.iaea.org>

[37] O.Iwamoto, *J.Nucl.Sci.Tech.* 45(9) (2008) 910-919

[38] A.Tudora, G.Vladuca, B.Morillon, *Nucl.Phys.A* 740 (2004) 33-58

[39] EXFOR Nuclear Data Base (2013). Target Th-230, reaction (n,f), quantity MFQ, Prompt Nu. Available on-line <http://www-nds.iaea.org>

[40] A.Tudora, B.Morillon, F.-J.Hambsch, G.Vladuca, S.Oberstedt, *Nucl.Phys.A* 756 (2005) 176-191

[41] EXFOR Nuclear Data Base (2013). Target Th-232, reaction (n,f), quantity E. Available on-line <http://www-nds.iaea.org>

Nuclear Data Section
International Atomic Energy Agency
Vienna International Centre, P.O. Box 100
A-1400 Vienna, Austria

E-mail: nds.contact-point@iaea.org
Fax: (43-1) 26007
Telephone: (43-1) 2600 21725
Web: <https://www-nds.iaea.org>
